

TREVERSE: TRial-and-ERror Lightweight Secure ReVERSE Authentication with Simulatable PUFs

Yansong Gao, Marten van Dijk, Lei Xu, Wei Yang, Surya Nepal, and Damith C. Ranasinghe

Abstract—A physical unclonable function (PUF) generates hardware intrinsic volatile secrets by exploiting uncontrollable manufacturing randomness. Although PUFs provide the potential for lightweight and secure authentication for increasing numbers of low-end Internet of Things devices, practical and secure mechanisms remain elusive. We aim to explore simulatable PUFs (SimPUFs) that are physically unclonable but efficiently modeled mathematically through privileged one-time PUF access to address the above problem. Given a challenge, a securely stored SimPUF in possession of a trusted server computes the corresponding response and its bit-specific reliability. Consequently, naturally noisy PUF responses generated by a resource limited prover can be immediately processed by a one-way function (OWF) and transmitted to the server, because the resourceful server can exploit the SimPUF to perform a trial-and-error search over likely error patterns to recover the noisy response to authenticate the prover. Security of trial-and-error reverse (TREVERSE) authentication under the random oracle model is guaranteed by the hardness of inverting the OWF. We formally evaluate the TREVERSE authentication capability with two SimPUFs experimentally derived from popular silicon PUFs.

Index Terms—PUF, simulatable PUF, trial-and-error, lightweight authentication, reliability confidence, server-aided.



1 INTRODUCTION

Physical unclonable functions (PUFs) exploit manufacturing imperfections to extract hardware instance-specific secrets on demand. The unavoidable fabrication variations of devices endows a PUF with physical unclonability. Thus, even the same manufacturer is incapable of forging two PUFs exhibiting identical behaviors. As a function, the PUF takes inputs (challenges) and react with instance-specific outputs (responses) referred to as challenge-response pairs (CRPs). The first silicon PUF, coined the Arbiter PUF [1] was created in 2002. Since then, various other microelectronic PUF types such as ring oscillator PUF (ROPUF) [2]–[4], SRAM PUF [5], [6], DRAM PUF [7]–[9], and nanoelectronic PUFs [10] have emerged. Primarily, PUF primitives are a fundamentally different solution to addressing the secure key storage problem

and authentication [2], [11]–[13]. In contrast to requiring of the secure non-volatile memory (NVM) to permanently store a the key in digital form, a PUF key is volatile and only present on demand. As a consequence of the ability to derive hardware intrinsic secrets, PUF primitives provide the potential for building authentication mechanisms with inherent key protection [2], [11], [14].

Realizing a lightweight authentication mechanisms with PUFs is a non-trivial task in practice. As a comprehensive examination of lightweight authentication mechanisms by Delvaux *et al.* [12], [15], [16] highlighted the difficulty of realizing PUF based authentication that is lightweight, secure and practical. A key hurdle is the naturally noisy nature of PUF responses. Most studied and popular silicon PUFs yield responses susceptible to thermal noise and environmental parameter fluctuations such as supply voltage and temperature. Therefore, PUF primitives must directly deal with noise inherent to the source of entropy used for deriving keys [2], [12], [17]–[24] (as detailed in Section 8). Consequently:

Realizing secure, lightweight and practical authentication in the presence of noisy PUF responses remains an open problem.

We observe that previous studies have established the challenge-response specific nature of PUF response reliability [25]–[28]. In essence, the homogeneous application of a reliability measure such as bit error rate across the entire challenge-response space presents only a limited characterization of response unreliability and ignores the challenge-response specific nature of unreliability. Following this observation, we unfold a new method in cryptography and security in this paper, so-called TREVERSE—trial and error authentication method where:

- 1) The resourceful server authenticates a prover exploiting

- Yansong Gao, Lei Xu and Wei Yang are with School of Computer Science and Engineering, Nanjing University of Science and Technology (NJUST), Nanjing, China. Yansong Gao is also with Data61, CSIRO, Sydney, Australia. yansong.gao@njjust.edu.au; xulei_marcus@126.com;generalzyzy@gmail.com
- Marten van Dijk is with Secure Computation Laboratory, Department of Electrical and Computer Engineering, University of Connecticut, USA. marten.van_dijk@uconn.edu
- Surya Nepal is with Data61, CSIRO, Sydney, Australia. surya.nepal@data61.csiro.au
- Damith C. Ranasinghe is with Auto-ID Labs, School of Computer Science, The University of Adelaide, SA 5005, Australia. damith.ranasinghe@adelaide.edu.au
- Usage Permission goes to IEEE. Cite as: Yansong Gao, Marten van Dijk, Lei Xu, Wei Yang, Surya Nepal, and Damith C. Ranasinghe. "TREVERSE: Trial-and-error Secure Lightweight Reverse Authentication with Simulatable PUFs." IEEE Transactions on Dependable and Secure Computing (2020).

its unique ability to *estimate the bit specific nature* of PUF response reliability together with its response.

- 2) The prover is oblivious to the noisy nature of the PUF response and treats the PUF response as a secure digital key; as in a classical crypto system without applying error correction.
- 3) The adversary is forced to build a method to discover *both* the bit specific reliability and the response information hidden from an adversary in a computationally intractable problem—a trapdoor function.

1.1 Goals and Contributions

The aim of this study is to investigate a new methodology¹ to achieve a secure and lightweight authentication implementation on a PUF embedded device—referred to as prover—in the presence of noisy PUF responses. Our authentication mechanism takes advantage of response-specific nature of PUF reliability and outsources the overhead of dealing with noisy nature of PUF responses from the prover to the server; here, we rely on the fact that the computational power can be flexibly configured at the server. Overall, our work makes the following contributions:

- We propose TREVERSE authentication. We challenge the commonly employed approach for dynamic authentication with PUFs where response bits are either: i) corrected using stored or sent helper to the prover; or ii) hashed response value generated on the prover and sent to the server is used to reconcile noisy response bits. Although counter to intuition, we directly employ *noisy* PUF responses without error correction or helper data generation.
- To the best of our knowledge, we are the first to develop a generic PUF based authentication mechanism, where: i) the PUF integrated device can be oblivious to the noisy nature of the PUF response; and ii) the PUF responses are directly employed for security functions, similar to a digital key stored in a secure NVM in a classical crypto system, without applying error correction.
- In order to realize TREVERSE, we propose a server-aided trial and error authentication algorithm, where the goal of the server is to recover the noise corrupted PUF response processed by a OWF on the prover. The capability is only held by the server because of a securely managed SimPUF that estimates *both* PUF responses and their bit specific reliability.
- We develop two sets of TREVERSE protocols: i) unilateral authentication; and ii) mutual authentication. We evaluate the security of these protocols, in particular, against *all* known modeling attacks. We show that TREVERSE authentication mechanisms are secure in the random oracle model.
- We validate the authentication capability and practicability of TREVERSE authentication through concrete formal analyses, and further extensive empirical experiments based on Virginia Tech’s public silicon PUF dataset [29].

1. We contrast our approach with existing methodologies in detailed in Section 8.

1.2 Paper Organization

Followed by an overview of TREVERSE in Section 2, we illustrate the existence of simulatable PUFs and techniques for enrolling SimPUFs in Section 3. In Section 4, we elaborate on the TREVERSE instantiation on the prover and then analyze its security. Section 5 concretely formalizes the TREVERSE authentication capability with respect to both false rejection rate and false acceptance rate. We also validate the formula based on empirical results. Based on public silicon PUF dataset, Section 6 experimentally evaluates authentication capability of TREVERSE from two different PUF types: ROPUF and linear additive PUF (LAPUF). In Section 7, we compare TREVERSE with other existed works and further discuss TREVERSE. In Section 8, we present related works, followed by conclusion in Section 9.

2 TREVERSE OVERVIEW

Here we denote binary vectors with a bold lowercase character, e.g., challenge \mathbf{c} and response \mathbf{e} . All vectors are row vectors. A set is denoted with calligraphic character, e.g., challenge set \mathcal{C} and response set \mathcal{E} . A procedure or function is printed in a sans-serif font, e.g. PUF(\mathbf{c}).

Consider the dynamic authentication scenario realized with a key derived from a prover integrated PUF illustrated in Fig. 1. For simplicity, we start by assuming that a hard-wired or fixed PUF challenge \mathbf{c} (not shown) is employed to derive a fixed response $\tilde{\mathbf{e}}$ on the prover. Following [12], we define a physical PUF and One-Way Function (OWF) as below.

Definition 1. PUF: For a given manufacturing process, a PUF is a manufactured building block that realizes a non-deterministic mapping from a set $\mathcal{C} \in \{0, 1\}^\lambda$ to a set $\tilde{\mathcal{E}} \in \{0, 1\}^\eta$, where the distribution of each random variable \tilde{e}_i , with $i \in [1, |\mathcal{C}|]$, depends on process variations, noise, environmental variables, and aging. Therefore, two random evaluations of the response given the same challenge might slightly vary but with an upper bound $\text{HD}(\mathbf{e}, \tilde{\mathbf{e}}) \leq \text{th}$, with threshold th a constant.

In general, assuming that the PUF is a function, given input challenge \mathbf{c} , it returns output response $\mathbf{e} \leftarrow \text{PUF}(\mathbf{c})$.

Definition 2. One-Way Function A function OWF is one-way if and only the function can be computed by a polynomial time algorithm, but any polynomial time randomized OWF⁻—pseduo-inverse function of OWF that attempts to compute a pseduo-inverse for OWF succeeds with negligible probability.

We refer to those PUFs that can be simulated, for example, using a mathematical model or exhaustive characterization where the characterization complexity is linear with respect to the number of challenges, as simulatable PUFs. The server in Fig. 1 holds a SimPUF(.); a parameterized model of the simulatable physical PUF embedded within the prover. We formally define a SimPUF below.

Definition 3. Simulatable PUF:² A PUF with a parameter-

2. We are aware that the term Simulatable PUF was previously used by Ruhrmair *et. al* in 2013 [30]. In general, the Simulatable PUF in [30] emulates only the response. This concept, while similar, is limited for our needs since the simulatable PUFs we describe predict the bit-specific reliability as well as the response.

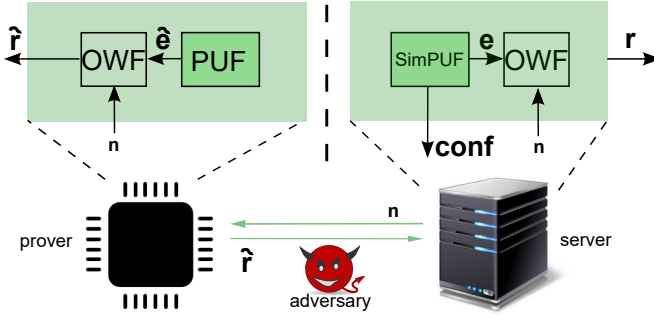


Fig. 1. TREVERSE considers three parties: the server, the prover and the adversary. The server holds a SimPUF that is a parameterized model of the physical PUF to not only accurately emulate the response e but also its corresponding reliability confidence conf .

ized model SimPUF capable of computing a response e and its corresponding reliability confidence conf in polynomial time for any given challenge c is said to be a simulatable PUF. Here: i) $(e, \text{conf}) \leftarrow \text{SimPUF}(c)$ where SimPUF is constructed using one-time privileged access by an authorized party in a secure environment and subsequent acquisition of SimPUF by any party is disabled; ii) e is indistinguishable from the response $\tilde{e} \leftarrow \text{PUF}(c)$, that is $\mathbb{P}(\tilde{e} = e)$ is ϵ -close to 1; and iii) the estimated conf is ϵ -close to the reliability confidence of \tilde{e} .

In the TREVERSE authentication scenario in Fig. 1, a SimPUF is held by the server. Subsequent acquisition of SimPUF by any party is disabled, for example, by fusing the access wire to the PUF response [31]. The TREVERSE authentication protocol can be described as follows:

- 1) A nonce n is issued by the server and sent to the prover³.
- 2) At the prover, an output $\tilde{r} \leftarrow \text{OWF}(\tilde{e}, n)$ is generated based on PUF response $\tilde{e} \leftarrow \text{PUF}()$ and the n . The prover transmits \tilde{r} to the server.
- 3) The server securely manages the SimPUF and computes e and the corresponding reliability confidence conf where $(e, \text{conf}) \leftarrow \text{SimPUF}()$.
- 4) Given conf , the server has the exclusive ability to identify bits that are least reliable in the response e . These bits will have a high chance to be different from that in \tilde{e} . The server exhaustively tries all error patterns for these unreliable bits to form a set of trial responses \mathcal{E}^t . The server successfully authenticates the prover if for any trial response $e^t \in \mathcal{E}^t$, $\text{OWF}(e^t, n) = \tilde{r}$, otherwise, the authenticity of the prover is rejected.

In general, the TREVERSE authentication relies on the server's *unique* ability to discover the response \tilde{e} according to their securely managed knowledge of SimPUF—detailed in Section 4.1. Notably, the adversary is forced to build a method to discover *both* the bit specific reliability information and the response information obfuscated from an adversary in a computationally intractable trapdoor function. The TREVERSE inevitably raises three important questions:

3. Notably, the nonce n may also be generated by the prover and sent to the server as in our TREVERSE-B instantiation, in Section 4.2.2, to allow the use of LAPUFs and/or mutual authentication functions.

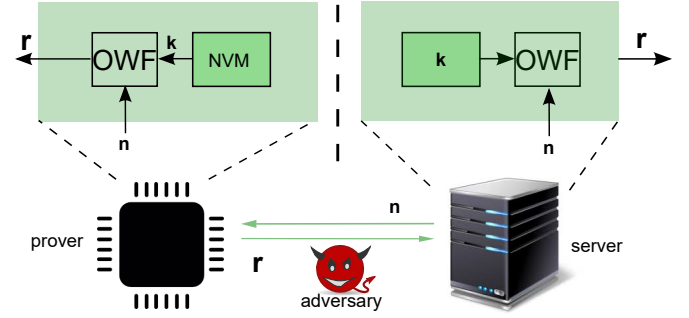


Fig. 2. Classical entity/client digital key based authentication. The key is commonly stored on the secure NVM.

- Do simulatable PUFs defined in Definition (3) exist in practice?
- What is the probability of false acceptance and false rejection—we refer to as the *authentication capability*—with respect to the number of unreliable response bits selected to generate the trial response set \mathcal{E}^t ?
- What is the security of the proposed protocol?

The following of this paper answers these questions.

3 SIMULATABLE PUFs

In practice, any PUF with the ability to exhaustively and repeatedly readout CRPs and associated bit-specific reliability in polynomial time can be a simulatable PUF. Unsurprisingly, PUFs with CRPs exponential in the number of challenge bits capable of being mathematically modeled also fall into the class of Simulatable PUFs. Without loss of generality, we elaborate on techniques to acquire a SimPUF for three different and popular silicon PUFs suitable for microelectronic devices: i) Linear Additive delay PUFs (LAPUFs); ii) ROPUFs; iii) and SRAM PUFs. The first one is a strong PUF owing to its exponential CRP space [32] while the later two are examples of weak PUFs with limited CRP space while the Recall that a SimPUF must be capable of estimating for any given challenge: i) the response; and ii) the associated bit specific reliability.

3.1 Linear Additive PUF

A popular PUF topology is the linear additive PUF (LAPUF) [22], [33], [34]. Representatives of the LAPUF are the Arbiter PUF (APUF) and the k -sum ROPUF [22], [33]. LAPUFs yield a massive number of CRPs in a limited area footprint in silicon.

Response: For LAPUFs, it is impractical to exhaustively readout its responses due to its very large CRP space. From a modeling perspective, the APUF and the k -sum ROPUF can be reduced to the same topology [22]. It has been widely shown that LAPUFs can be modeled [32], [35]–[38]. TREVERSE authentication benefits from the existing body of methods for constructing a mathematical model of an LAPUF. The server can learn LAPUF model parameters using a limited number of direct CRP measurements during the secure enrollment phase to subsequently emulate the response of any chosen challenge.

Bit specific reliability: In fact, an LAPUF model is not only able to emulate the response to a given a random challenge, it can also be employed to accurately predict the bit-specific reliability of the response [39]. To be precise, given a challenge, the LAPUF model predicts a numerical value that is linear with the time difference between the top and bottom paths in the APUF, or frequency difference between the top and and bottom paths in the k -sum ROPUF. Such an numerical value can be utilized as the bit-specific reliability. As for the binary response, if the value is larger than zero, then the predicted response is ‘1’, otherwise ‘0’.

3.2 Ring Oscillator PUF (ROPUF)

An ROPUF has a number, k , of ring oscillators (ROs); each RO has an odd number of inverters. The frequency of each RO is designed to be identical but varying in practice due to fabrication randomness. The ROPUF produces a response upon comparing frequencies of a pair of ROs where the given challenge selects the pair to be compared [2].

Response: The ROPUF also has a limited CRP space. Specifically, the number of CRPs is $\lfloor \frac{k}{2} \rfloor$ when a response is produced from independent ROs and $\binom{k}{2}$ when the response generated from all possible combinations of ROs. Therefore, the responses can be fully characterized by the server.

Bit specific Reliability: The response bit-specific reliability can be evaluated conveniently by subtracting the frequencies of the two ROs selected by a given challenge. The magnitude of the difference in the frequencies can then be employed to estimate the reliability of the response bit [40].

3.3 SRAM PUF

The SRAM PUF exploits random but repeatable power-up states of SRAM cells as responses; each cell consists of two cross-coupled inverters, where the cell address is the challenge [5].

Response: Given the limited CRP space of a SRAM PUF, an exhaustive readout of CPRs can be performed by the server to enroll response bits.

Bit specific reliability: To gain a bit-specific reliability model, current methods is to apply multiple physical measurements of the same SRAM PUF response. The number of measurements is in the order of 10 to 100 [25], [41] that has been shown to be applicable to the soft-decision based error correction. More number of measurements performed, more accurate the bit-specific reliability ⁴.

4 TREVERSE AUTHENTICATION

We presented an overview of TREVERSE authentication in Section 2. In this section, we begin with a description of the algorithm employed by a server. Then we detail both TREVERSE unilateral and mutual authentication along with specific prover architectures and analyze the security.

	Response	Confidence	Ranking
e_1	x	-0.012	2
e_2	x	-0.140	3
e_3	1	+0.482	5
e_4	0	-0.660	6
e_5	x	+0.007	1
e_6	0	-1.100	7
e_7	1	+0.230	4
e_8	1	+1.634	8

Fig. 3. An example of sorting reliability confidence of responses. Lower the reliability (closer to zero), higher the ranking. The highest ranked $m-m = 3$ for example—response bits are marked as unknown, because their regenerations, e.g., $\tilde{e}_5, \tilde{e}_1, \tilde{e}_2$, are more likely to be flipped and thus differing from e_5, e_1, e_2 .

4.1 Trial and Error Authentication

We take a motivating example to help describe the algorithm 1 for trial and error conducted by a server. Assuming that for a chosen challenge c , the server employs its SimPUF to compute the response $e = \{e_1, \dots, e_8\}$, a response bit vector of length $k = 8$, with the associated response bit confidence as shown Fig. 3. Here, an **index** vector ranks each response bit’s reliability in descending order; lower the reliability, higher the ranking. For example, $index_1$ corresponds to e_5 and $index_2$ corresponds to e_1 . Then for m lowest confidence bits where $m < k$, response bits $e_{index_1}, \dots, e_{index_m}$ are selected as m unreliable response bits.

In order to conduct trial and error authentication, the server can exhaustively iterate over all possible error patterns for these m unreliable response bits, $e_{index_1}, \dots, e_{index_m}$. The $k-m$ reliable response bits emulated using the SimPUF is kept unaltered during this trial and error phase.

To illustrate the algorithm, suppose that the prover generated response \tilde{e} is “01100011”. Then, consider for the enrolled response shown in Fig. 3, the selected number of lowest confidence bits $m = 3$. Consequently, the server can generate the possible set of error patterns $\{0,0,0; 0,0,1; 0,1,0; 0,1,1; 1,0,0; 1,0,1; 1,1,0; 1,1,1\}$ for e_5, e_1 and e_2 . Each error pattern is injected into the unreliable response bit positions 5, 1, and 2 to form a trial response $e^t \in \mathcal{E}^t$. Subsequently, the server iterates over all $e^t \in \mathcal{E}^t$ to compute the corresponding response r^t and compares with the received response \tilde{r} from the prover. Suppose the server tries each error pattern sequentially, we can see that within two trials, the authenticity of the token is accepted. Notably, in the worst case, *at most*, $2^m = 8$ trials are performed with $m = 3$. If *all* the trials fail, the authenticity of the token is rejected.

4.2 Unilateral Authentication

We have established a method for trial and error authentication by a server. Now, we consider the realization of unilateral authentication with a simulatable PUF on a prover. We propose two prover architectures that we refer to as: i) TREVERSE-A; and ii) TREVERSE-B.

4.2.1 TREVERSE-A

We propose TREVERSE-A illustrated in Figure 4 as a prover architecture, which is comparable with a prover implemen-

⁴ Exhaustive repeated measurement is possible but is not preferable in practice. Therefore, new methods to gain accurate bit-specific reliability of the SRAM PUF without relying on exhaustive repeated measurement as an interesting future work should be investigated.

Algorithm 1 TREVERSE authentication

```

1:  $\tilde{\mathbf{r}}$   $\triangleright$  received response vector from the token
2:  $\mathbf{n}$   $\triangleright$  nonce employed in the protocol
3:  $[\mathbf{e}, \mathbf{conf}]$   $\triangleright$  generated using the securely held SimPUF
4:  $[\mathbf{index}] = \text{sort}(\text{abs}(\mathbf{conf}), \text{'ascending'})$   $\triangleright$   $\text{sort}()$  is a
   sorting function,  $\text{abs}(x)$  is a function returning the absolute
   value of  $x$ 
5: procedure authenticate ( $\mathbf{e}, \tilde{\mathbf{r}}, \mathbf{index}$ )
6:    $\text{authState} \leftarrow \text{Fail}$ 
7:   for  $i = 1 : 2^m$  do
8:     generate a new trial response  $e_i^t$  by altering response
       bits  $e_{\text{index}(1)}, \dots, e_{\text{index}(m)}$ 
9:     compute response  $\mathbf{r}$  using  $e_i^t$  and  $\mathbf{n}$ 
10:    if  $\mathbf{r} = \tilde{\mathbf{r}}$  then
11:       $\text{authState} \leftarrow \text{Success}$   $\triangleright$  prover is authenticated
12:    return  $\text{authState}$ 
13:    end if
14:  end for
15: end procedure

```

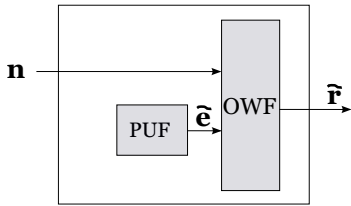


Fig. 4. TREVERSE unilateral instantiation, TREVERSE-A, on the prover. The nonce \mathbf{n} is sent by the server. PUF response is required to be iid, e.g., for the SRAM PUF and ROPUF with each RO used only once.

tation in the classical authentication using a digital key stored in the secure NVM—see Figure 2. We make two assumptions for PUFs that utilize this architecture.

- We assume the simulatable PUF on the prover generates responses that are information theoretically independent. In other words, each CRP is generated from a spatially separate physical structure.
- We assume that prover generated PUF response is from a hardwired and, therefore, fixed challenge.

Examples of Simulatable PUFs that are appropriate include the SRAM PUF and the ROPUF⁵. For instance, in ROPUF, we can generate $\lfloor \frac{k}{2} \rfloor$ independent response bits out of k ROs. These $\lfloor \frac{k}{2} \rfloor$ bits can be readout entirely as key material. For an SRAM PUF, a start address can be hardwired and the subsequent SRAM cells readout as the PUF response $\tilde{\mathbf{e}}$.

Protocol: The unilateral authentication protocol with TREVERSE-A as follows:

- 1) The server issues a nonce \mathbf{n} and transmits it to the prover.
- 2) The prover reads out the fixed PUF response $\tilde{\mathbf{e}}$ and transmits the output $\tilde{\mathbf{r}} = \text{OWF}(\tilde{\mathbf{e}}, \mathbf{n})$ to the server.
- 3) The server performs TREVERSE using Algorithm (1). If the server sees that the computed response

5. Recent work [12] takes initial steps into taking bias and spatial correlation into account e.g., for SRAM PUF [12] (Chapter 4.3.5) when evaluating the entropy loss bound of a PUF key generator. However, due to the complexity to formally develop an easy-to-use tight bound, the iid property of responses is commonly assumed for PUFs such as SRAM PUF and ROPUF.

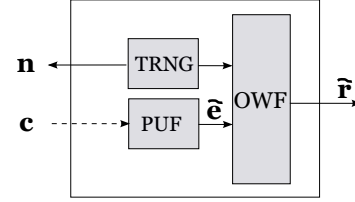


Fig. 5. TREVERSE unilateral instantiation, TREVERSE-B, on the prover. The nonce \mathbf{n} is generated by the prover and sent back to the server. There is no constraint on the PUF property. The dotted arrow means that the $\tilde{\mathbf{e}}$ can be refreshed by the server issued \mathbf{c} on demand, or the $\tilde{\mathbf{e}}$ can also be fixed given a fixed \mathbf{c} .

$\mathbf{r} \leftarrow \text{OWF}(\mathbf{e}^t, \mathbf{n})$ is identical to $\tilde{\mathbf{r}}$, the prover is considered authenticated by the server.

TREVERSE-A is, to the best of our knowledge, *the first PUF authentication instantiation that is same to the classical digital key based unilateral authentication illustrated in Fig. 2*. In the next section, we describe a prover PUF architecture that eschews the constraint on the PUF property necessary for TREVERSE-A.

4.2.2 TREVERSE-B

We propose the token architecture we refer to as TREVERSE-B to provide a generic prover implementation for any given simulatable PUF. The prover instantiation is depicted in Fig. 5. This architecture provides following advantages:

- It can be employed with various PUF types: LAPUFs, ROPUFs and SRAM PUFs. Although the later two are applicable to TREVERSE-A.
- It allows the server to refresh the prover response or secret according to the server issued challenge \mathbf{c} on demand between sessions to benefit from the large CRP space of PUFs such as LAPUFs.
- It does not strictly require that PUF responses are information theoretically independent.

Protocol: The unilateral authentication protocol with TREVERSE-B follows:

- 1) The server issues a challenge \mathbf{c} and transmits it to the prover.
- 2) The prover applies \mathbf{c} to gain the PUF response $\tilde{\mathbf{e}}$ where $\tilde{\mathbf{e}} \leftarrow \text{PUF}(\tilde{\mathbf{c}})$. The prover TRNG generates a nonce \mathbf{n} . Then the prover transmits output $\tilde{\mathbf{r}} \leftarrow \text{OWF}(\tilde{\mathbf{e}}, \mathbf{n})$ and the nonce \mathbf{n} to the server.
- 3) The server performs TREVERSE using Algorithm 1. If the server computed response $\mathbf{r} \leftarrow \text{OWF}(\mathbf{e}^t, \mathbf{n})$ is identical to $\tilde{\mathbf{r}}$, the prover is considered authenticated by the server.

Considering that a PUF generally produces a 1-bit response to a given challenge, a linear feedback shift register (LFSR) or a monotonic counter can be utilized to expand a seed challenge \mathbf{c} into required number of challenges to obtain a k -bit response $\tilde{\mathbf{e}}$. The nonce generator on a token can be a true random number generator (TRNG) or a well designed pseudo random generator (PRNG) such as the one employed by Yu *et al.* [31]. The TRNG can be derived from available PUF resources via unreliable PUF responses [42]–[46], for example, from APUFs [42], ROPUFs [46] and SRAM

PUFs [43], [44]. Notably, as we will discuss in Section 7, most of secure state-of-the-art PUF based authentication mechanisms rely on a TRNG.

4.3 Mutual Authentication

The TREVERSE-B prover architecture also enables mutual authentication by adding several steps, as detailed below.

Protocol: The mutual authentication protocol with TREVERSE-B:

- 1) The server issues a challenge c and transmits it to the prover.
- 2) The prover applies challenge c to readout PUF response \tilde{e} where $\tilde{e} \leftarrow \text{PUF}(c)$. The prover TRNG generates a nonce \mathbf{n}_1 . Then the prover transmits output $\tilde{r} \leftarrow \text{OWF}(\tilde{e}, \mathbf{n}_1)$ and the nonce \mathbf{n}_1 to the server.
- 3) The server performs TREVERSE using Algorithm 1. If the server computed response $\mathbf{r} \leftarrow \text{OWF}(e^t, \mathbf{n}_1)$ is identical to \tilde{r} , the prover is considered authenticated by the server otherwise the session is aborted.
- 4) The server acknowledges the prover if accepted. The prover issues nonce \mathbf{n}_2 and transmits it to the server and computes a $\tilde{r}_2 \leftarrow \text{OWF}(\tilde{e}, \mathbf{n}_2)$.
- 5) Upon receipt of nonce \mathbf{n}_2 , the server computes $\mathbf{r}_2 \leftarrow \text{OWF}(e^t, \mathbf{n}_2)$, and transmits \mathbf{r}_2 to the prover. Here, $e^t = \tilde{e}$ by way of step 2 in the protocol.
- 6) The prover accepts the authenticity of the server if and only if $\tilde{r}_2 = \mathbf{r}_2$, otherwise the server is rejected and the mutual authentication is aborted.

4.4 Security Analysis

We have looked at the problem achieving classical dynamic authentication and mutual authentication with noisy PUFs. We analyze the security of TREVERSE protocols in the archetypal setting of two parties communicating over an insecure channel attempting to authenticate each party. The two parties are attempting to achieve the security task of authentication or mutual authentication using the insecure communication medium via a TREVERSE protocol.

4.4.1 Adversary Model

We adopt an adversary model commonly used with analyzing PUF based security mechanisms [23], [31], [32], [36]. In summary: i) an adversary is allowed to eavesdrop on the communication channel; and ii) arbitrarily apply challenges via the publicly accessible interface to observe the prover response \tilde{r} . We assume that SimPUF enrollment is performed by the server in a secure environment using one-time privileged access and such access is prohibited afterwards. As in previous work [23], [31], [32], [36], we focus on brute-force attacks, replay attacks, and modeling attacks. We also discuss physical attacks.

4.4.2 Brute-force Attacks

The probability of correctly guessing a k -bit response \tilde{e} is expressed as:

$$\mathbb{P} = (\max\{\tau, 1 - \tau\})^k \quad (1)$$

where the τ is the response bias—to be ‘1’/‘0’. Notably, modern PUFs usually have low bias where τ is normally

close to 0.5 [47]. The LAPUF evaluated in this work has a τ of 50.05%. We can see that when k is larger than, e.g., 80, the brute-force attack success probability becomes extremely small. Therefore, brute-force attacks are extremely unlikely to succeed.

4.4.3 Replay Attacks

In a replay attack scenario, an adversary attempts to authenticate a fraudulent prover to the server by exploiting previously recorded information from protocol sessions. First, consider TREVERSE-A architecture based protocols. The nonce sent by the server is refreshed each session to prevent replay attacks. Second, in TREVERSE-B architecture based protocols, the nonce generated by the token is refreshed for each session; Therefore, replay attacks are prevented.

4.4.4 Modeling Attacks

Essentially, modeling attacks are dependent on the type of PUFWeak PUFs such as ROPUFs and SRAM PUFs with information theoretically independent responses are inherently immune from modeling attacks [32]. As a consequence, both TREVERSE-A and TREVERSE-B when employing these PUFs are immune to modeling attacks. However, PUFs with responses that are correlated with each other, are potentially vulnerable to modeling attacks. A typical characteristic of this PUF type is a very large CRP space provided with limited implementation area. Therefore, such PUF is related to the TREVERSE-B prover architecture. Specifically, we consider most studied LAPUFs.

In the TREVERSE-B instantiation, the response \tilde{e} is hidden behind the OWF trapdoor function. Therefore, conventional modeling attacks exploiting, for example, support vector machine (SVM) and logistic regression (LR) machine learning algorithms [32], [36] needing access to both challenge c and response \tilde{e} are prevented. Reliability based modeling attacks that exploit reliability information of CRPs, where a direct relationship between a challenge and a response is no longer required [37] are also prevented. This is because an adversary is unable to discover bit-specific reliability information. Attempts to ascertain bit specific reliability information of a challenge-response pair will not succeed since the on-chip nonce prevents inferring the reliability of a PUF response \tilde{e} by observing the output \tilde{r} . Therefore, all known modeling attacks are inapplicable to the TREVERSE-B instantiation. Interestingly, based on the above analysis, we can also conclude that the bit-specific reliability information as well as the PUF response in a TREVERSE-B instantiation is hidden from an adversary in a computationally intractable problem—a trapdoor function.

Notably, composite PUFs, especially those built upon the APUF [48], [49], can increase modeling attack resilience without using an OWF construct as in TREVERSE. Although these composite PUFs can be adopted as a device PUF because TREVERSE is independent of the underlying device PUF type as long as a simulatable PUF can be obtained, composite PUFs usually result in more noisy response bits. Therefore using a composite PUF will increase the number of unreliable responses TREVERSE is required to trial. As TREVERSE by design relying on an OWF to prevent modeling attacks, a common LAPUF instead of a composite PUF built upon LAPUFs is more preferable to avoid the need

to deal with an unnecessarily high number of unreliable response bits.

4.4.5 Invasive attacks

Although we do not specifically consider a single PUF construction but describe TREVERSE as a new lightweight method for PUF based authentication, we report on potential invasive attacks and highlight countermeasures as well as the difficulty of mounting such attacks on PUFs. In comparison with digitally stored keys, a PUF provides inherent tamper resistance to invasive attacks in comparison with keys stored in NVM [2], [11], [15]. The key material hidden in the physical structure of PUF circuitry is harder to readout compared to keys stored in NVM. In addition, the process of tampering can destroy a PUF.

An attacker delayering the IC (integrated circuit) and probing PUF circuits to extract information to construct derived PUF secrets is harder without affecting the PUF CRP behavior or even destroying it once the PUF layout is constructed carefully. One example of such construction proposal is the controlled PUF [50], [51] with a control logic and an APUF where the APUF prevents invasive attacks on the control logic and the control logic protects the APUF from protocol level attacks, and another experimentally validated construction is the capacitive PUF [52], [53]. For hybrid attacks combining timing and power side channel information with machine learning usually requires on-chip peripheral circuits [54] to measure side channel information of the response. However, those circuits appear to be unavailable in resource-constraint devices. In addition, these attacks can be eliminated through careful circuit design techniques, e.g., dynamic and differential CMOS logic [54]. More importantly, the required power and timing measurement on a directly exposed LAPUF response e in [54] is prevented in a TREVERSE-A or TREVERSE-B prover architecture, because the response e is now hidden from an adversary through the transformation through the one way function OWF. Attacks using photonic side channel information [55] requires specialized laboratory equipment and professional skills; such photonic emission based attacks can be eliminated by circuit design techniques such as the use of interconnect meshes [56].

5 FORMALIZING AUTHENTICATION CAPABILITY

The TREVERSE authentication inevitably leads to the question of investigating the two important capabilities: i) the false acceptance rate (FAR)—the probability of the server accepting an illegitimate prover; and ii) false rejection rate (FRR)—probability of falsely rejecting a legitimate prover. In the following, we formally derive these metrics by considering a bit specific reliability model.

5.1 False Acceptance Rate

The TREVERSE authentication has zero tolerance for errors outside the $k - m$ reliable response bits bound. Recall, that after each trial response e^t construction, the server employs an exact match criterion; that is $\bar{e}^t = e$. Thus, for a given m highly unreliable bit selections and k PUF response bits, at most m bits in fixed positions can be different from the

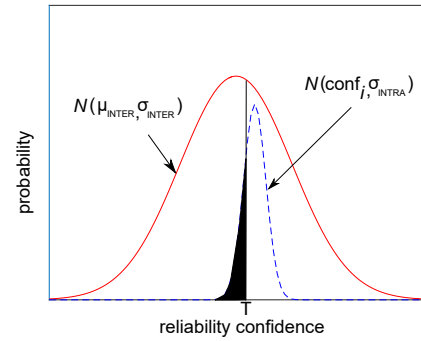


Fig. 6. Probability density of reliability confidence information. The solid red curve is the reliability confidence distribution of a large population of response bits during enrollment. Ideally, this follows the normal distribution $N \sim (\mu_{\text{INTER}}, \sigma_{\text{INTER}})$. The dashed blue curve is the probability density distribution of reliability confidence of a given bit under different environmental conditions and over multiple evaluations; this distribution is modeled as a normal distribution $N \sim (\text{conf}_i, \sigma_{\text{INTRA}})$.

server enrolled response. Therefore, FAR can be expressed as the probability of any other token generating $k - m$ bits of a given token to a chosen challenge c . Given response bias τ , FAR can be evaluated as:

$$\text{FAR} = (\max\{\tau, 1 - \tau\})^{k-m} \quad (2)$$

Supposing that the $k - m$ is large—it is indeed the case, e.g., up to 80 according to our evaluation in Section 6, this success is extremely small in practice.

5.2 False Rejection Rate

A legitimate prover response is falsely rejected by a server if at least one of $k - m$ bits of a PUF response \bar{e} from a legitimate token mismatch with the selected $k - m$ bits of the enrolled response e at the server—see Algorithm (1). Then, we can see that formally deriving an accurate false rejection rate requires a model of the response error distribution capable of capturing the bit specific nature of response reliability. The error distribution will allow us to estimate the probability of at least one of $k - m$ bits of a legitimate PUF response \bar{e} mismatching with the $k - m$ bits of the enrolled response e at the server.

Inferencing error probabilities based on a bit specific reliability model can be found in prior studies [25]–[27]. We will use the formulation in [27] to build a response model as in [25], [26] because we want a method of relating the bit response model to physical variables that can be directly observable and measurable: in particular, the confidence information of a bit.

Response Model: We describe a PUF response using the response confidence information. We let the random variable $\mathcal{C}_{\text{enroll}}$ represent the response reliability confidence from which a value conf_i is obtained for a given PUF response during enrollment. For a population of response bits e , we assume the random variable $\mathcal{C}_{\text{enroll}}$ is described by $N \sim (\mu_{\text{INTER}}, \sigma_{\text{INTER}})$. We illustrate this distribution in Fig. 6. Our assumption of normality is validated in the experimental results presented in [25]–[27]. When a PUF response is reevaluated, operating conditions such as

electrical noise influence the measurement. We model this noise using the random variable \mathcal{N} . When a response e_i is reevaluated at the j -th instance, a value $n_i^{(j)}$ sampled from \mathcal{N} influences the confidence information of a bit. We define a reevaluated bit response e_i as follows ⁶:

$$\tilde{e}_i = \begin{cases} 1 & \text{if } \text{conf}_i + n_i^{(j)} < T \\ 0 & \text{else} \end{cases} \quad (3)$$

with T a threshold parameter. In practice, this T is usually set to be 0. For example, in ROPUF, if subtraction of two ROs frequencies is lower than 0, then producing response '1', otherwise, '0'. In APUF, if time difference between top and bottom is lower than 0, then producing response '1', otherwise, '0'. Therefore, following this common empirical setting, we set the threshold T to be 0 henceforth.

Here we assume \mathcal{N} is a normal distribution described by $N \sim (\mu_{\text{INTRA}}, \sigma_{\text{INTRA}})$. The assumption of normality we employ is experimentally validated in [25], [26]. Notably, the response model we follow is described in [25], [26] with the exception that we define a response model based on using bit confidence information.

Response Distribution: Then for a response e_i we define the one-probability—Eq. (2) in [25], the probability of response \tilde{e}_i being one under the j th reevaluation—is defined as:

$$p_{\tilde{e}_i} = \Pr(\tilde{e}_i^{(j)} = 1) \quad (4)$$

Considering our definition of response bit in (3) under the assumption of a normal distribution for \mathcal{N} , we can write the one-probability as:

$$p_{\tilde{e}_i} = \Phi\left(\frac{T - \text{conf}_i}{\sigma_{\text{INTRA}}}\right), \quad (5)$$

where Φ is the cumulative distribution function (CDF) of the standard normal distribution. The probability $p_{\tilde{e}_i}$ can be illustrated by the shaded region in Fig. 6. Here, $p_{\tilde{e}_i}$ of a given response is a sample from the random variable $P_{\tilde{e}}$ denoting the possible one-probability of all response bits. As in [25], [26], we define the CDF of $P_{\tilde{e}}$ as:

$$\begin{aligned} \text{CDF}_{P_{\tilde{e}}}(x) &= \Pr(p_{\tilde{e}} \leq x) = \Pr(P_{\tilde{e}} \leq x) \\ &= \Pr\left(\Phi\left(\frac{T - \mathcal{C}_{\text{enroll}}}{\sigma_{\text{INTRA}}}\right) \leq x\right) \\ &= \Phi(\lambda_1 \Phi^{-1}(x) + \lambda_2). \end{aligned} \quad (6)$$

In (6), $\lambda_1 = \frac{\sigma_{\text{INTRA}}}{\sigma_{\text{INTER}}}$ and $\lambda_2 = \frac{\mu_{\text{INTER}}}{\sigma_{\text{INTER}}}$. The T is set to be 0 in (6) for simplification, this setting actually always gives conservative estimation of the FRR. We are now able to express the one-probability of a population of response bits using four parameters that can be obtained from direct measurements. Recall in Section 3 we discussed the extraction of bit specific confidence information for different PUF types during enrollment. Consequently, we can obtain σ_{INTER} and μ_{INTER} from direct measurements. In [27], it was recognized that σ_{INTRA} and μ_{INTRA} can be measured from the distribution of change in confidence information

from enrollment with respect to a change in operating conditions. Consequently, $\Pr(\mathcal{C}_{\text{ref}} - \mathcal{C}_{\text{enroll}})$, where ref is the new operating condition, can be used to estimate the distribution parameters of \mathcal{N} .

Remark: To simplify the formalization of the Eq. (6), by assuming T to be 0, we have assumed the response is uniformly and randomly distributed—probability of being '1'/'0' is 50%. It's worth to mention that such an assumption provides a conservative assessment [27], which is indeed experimentally validated in Section 5.3.2.

Response Error Distribution: Now, we are able to find response error distribution based on the one-probability as described in [25], [26]. Recall that the enrolled response generated by a SimPUF is e and we assume this to be the correct response. Now, the error probability given a bit \tilde{e}_i reevaluated on the j th occasion can be defined as:

$$p_{\text{err}_i} = \Pr(\tilde{e}_i^j \neq e_i). \quad (7)$$

The error probability p_{err_i} given response \tilde{e}_i is a sample of a random variable P_{err_i} of a population of response bits. Then, the CDF of P_{err_i} can be defined and expressed as in [25], [26]:

$$\begin{aligned} &\text{CDF}_{P_{\text{err}}}(x) \\ &= \Pr(p_{\text{err}_i} \leq x) \\ &= \Pr(P_{\text{err}} \leq x) \\ &= \text{CDF}_{P_{\tilde{e}}}(x) + 1 - \text{CDF}_{P_{\tilde{e}}}(1 - x) \\ &= \Phi(\lambda_1 \Phi^{-1}(x) + \lambda_2) + 1 - \Phi(\lambda_1 \Phi^{-1}(1 - x) + \lambda_2). \end{aligned} \quad (8)$$

We illustrate response error distribution $\text{CDF}_{P_{\text{err}}}(x)$ using an example from ROPUF data. In Fig. 13⁷ in Appendix shows the $\text{CDF}_{P_{\text{err}}}(x)$ as a function of error probability x . One important observation we can obtain from the cumulative distribution $\text{CDF}_{P_{\text{err}}}(x)$ is the determination of the percentage of response bits satisfying a error probability of less than x . For example, just over 10% of responses have an error probability is less than 10^{-7} .

False Rejection Rate: The number of errors in a k -bit response no longer follows a binomial distribution but a Poisson-binomial distribution [26]. This is because the one-probability of a response bit is no longer constant and therefore cannot be modeled using a binomial distribution. Given k response bits, their error probabilities can be represented as $\mathbf{p}_{\text{err}} = (p_{\text{err}_1}, \dots, p_{\text{err}_k})$. As highlighted in [26], generating the random distribution of bit failures using the bit specific response error model is difficult to achieve analytically since it involves the k -dimensional distribution of \mathbf{p}_{err} . However, as demonstrated in [26], we are able to efficiently simulate k bit responses by randomly sampling k probabilities from the cumulative distribution $\text{CDF}_{P_{\text{err}}}(x)$ by using inverse transform sampling. Given TREVERSE authentication tolerates m most unreliable bits: i) we sort randomly derived \mathbf{p}_{err} in descending order and obtain $\mathbf{p}_{\text{err}}^S$; and ii) exclude the first m

⁶. Using $\tilde{e}_i = 1$ if $\text{conf}_i > T$ and $\tilde{e}_i = 0$ if $\text{conf}_i \leq T$ in (6) will yield the same results

⁷. Here, $\lambda_1 = 0.3231$ and $\lambda_2 = -0.3477$ are drawn from the measurements given in Table. 1.

elements in $\mathbf{p}_{\text{err}}^S$ with lowest reliability confidence to obtain $\mathbf{p}_{\text{err}}^{S(k-m)}$ with length of $k - m$. We can now express FRR as:

$$\text{FRR} = 1 - F_{\text{PB}}(t = 0; \mathbf{p}_{\text{err}}^{S(k-m)}), \quad (9)$$

with $F_{\text{PB}}(t; \mathbf{p}_{\text{err}}^{S(k-m)})$ the Poisson-binomial cumulative distribution function [26]. We use the setting $t = 0$ since $k - m$ bits must exhibit no errors. In practice, randomly sampling a large number (we use 1,000) of k -bit responses and repeatedly evaluating the corresponding sampled \mathbf{p}_{err} using (9) yield a large random sample of FRR. The mean of FRR of those evaluations is adopted.

5.3 Validating False Rejection Model

This section validates the bit-specific reliability model derived FRR by showing that the statistical FRR in (9) fits empirical results. The validations are from both ROPUF and LAPUF.

5.3.1 PUF dataset

There are three public ROPUF datasets: Virginia Tech [29], FPL2017 [57] and HOST2018 [58]. Both FPL2017 and HOST2018 are only evaluated under a limited range of operating conditions—only varying temperature; therefore, ROPUFs show a much lower worst-case unreliability ϵ : 3.57% for FPL2017 and 3.06% for HOST2018. In contrast, Virginia Tech ROPUFs exhibit a 9.66% worst-case ϵ . As we are interested in evaluating TREVERSE under a worst-case setting, we chose the older Virginia dataset for comprehensive validations and select the latest HOST2018 dataset for a complementary evaluation detailed in Appendix. C.

As for the Virginia ROPUF dataset, five ROPUFs are implemented across five Spartan3E S500 FPGA boards. Each FPGA implements one ROPUF that consists of 512 ROs. Details of the constructions are given in [29]. The dataset contains each RO's frequency measurements. Each RO frequency measurement is repeated 100 times under the operating voltages of 0.96 V, 1.08 V, 1.20 V, 1.32 V, and 1.44 V at a fixed temperature of 25°C to capture supply voltage influences. Similarly, each RO frequency is also evaluated 100 times under 35°C, 45°C, 55°C, and 65°C, with a fixed supply voltage of 1.20 V, to reflect influence from temperature changes.

5.3.2 Validation with an ROPUF

There are $\binom{512}{2} = 130816$ possible combinations to select a pair of ROs out of 512 ROs in one ROPUF⁸. Therefore, one ROPUF yields 130816 CRPs. The reliability of all five ROPUFs are evaluated. Worst unreliability will result in worst FRR, thus, we are interested in the ROPUF instance that exhibits the *worst* BER or ϵ , which is summarized in Table. 1 (second column) under varying operating conditions. The BER is dominantly influenced by the supply voltage, which is in well agreement with other reports [29].

The reliability confidence of the ROPUF is the frequency subtraction of the pairwise ROs. For all 130816 response bits,

8. Note that we can use each RO only once to extract a 256-bit response to make the response generation independent. The reason of not doing so here is to facilitate the experimental demonstration with a large CRP sample.

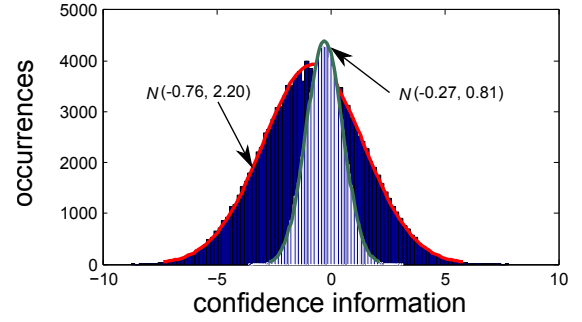


Fig. 7. Measured σ_{INTRA} and σ_{INTER} . The shown $\sigma_{\text{INTRA}} = 0.81$ is evaluated under the worst-corner (0.96 V, 25°C). While the $\sigma_{\text{INTER}} = 2.2$ is evaluated under nominal operating condition of (1.20 V, 25°C).

TABLE 1
 λ_1 and ϵ measured under different operating conditions and the λ_2 . Referenced operating condition is (1.20 V, 25°C).

Operating condition	ϵ	σ_{INTRA}	λ_1	λ_2
(25°C, 0.96 V)	9.66%	0.8006	0.3672	-0.3477
(25°C, 1.08 V)	4.68%	0.4248	0.1933	-0.3477
(25°C, 1.20 V)	0.98%	0.0523	0.0239	-0.3477
(35°C, 1.20 V)	1.82%	0.1627	0.0728	-0.3477
(45°C, 1.20 V)	1.88%	0.1569	0.0700	-0.3477
(55°C, 1.20 V)	2.08%	0.1741	0.0795	-0.3477
(65°C, 1.20 V)	2.17%	0.1933	0.0881	-0.3477
(25°C, 1.32 V)	4.70%	0.4729	0.2151	-0.3477
(25°C, 1.44 V)	6.42%	0.7182	0.3231	-0.3477

distribution of frequency subtraction of these response bits are evaluated under different operating conditions. Same to the observation in [27], the mean and variance of the distribution changes only slightly under differing operating conditions. Thus, the μ_{INTER} and σ_{INTER} measured under the nominal operating condition (1.20 V, 25°C) is used, as shown in Fig. 7. Notably, the μ_{INTER} is not ideally equal to 0 that thereby induces a severe bias, in particular, response '1' to be 36.65%. To measure σ_{INTRA} that is the variance introduced by including noise and voltage, temperature deviation from that of nominal operating condition, the frequency subtraction given all response bits are measured under the nominal operating condition (1.20 V, 25°C) treated as a *reference*, then frequency subtraction given all response bits are measured *again* under a deviating operating condition, e.g., (0.96 V, 25°C). The change between these two measurements is assessed. The standard deviation is recognized as σ_{INTRA} . In Fig. 7 the σ_{INTRA} evaluated under the worst-corner of (0.96 V, 25°C) is shown. Table. 1 lists $\lambda_1 = \frac{\sigma_{\text{INTRA}}}{\sigma_{\text{INTER}}}$ evaluated under different operating conditions and $\lambda_2 = \frac{\mu_{\text{INTER}}}{\sigma_{\text{INTER}}}$.

Results: Empirical and statistical results of FRR are shown in Table 2. They agree well. The FRR decreases as the m increases. In addition, the FRR is minimizing when the \tilde{e} is regenerated under an operating condition that is close to the nominal operating condition. In other words, *the FRR gets worse as σ_{INTRA} goes up.*

One may note that the statistical results show a conservative assessment of the FRR in comparison with the empirical results. The reason is that the response has a bias, response '1' to be 36.65%, in this ROPUF case. In other words, Confidence in Fig. 3 does not follow a normal distribution with a *mean value of zero*, instead μ_{INTER} deviates from zero, which explains the conservative assessments [27].

TABLE 2

FRR of the ROPUF under different operating conditions and m settings, where $k = 64$. Referenced operating condition is (1.2 V, 25°C).

m	25°C, 0.96 V	25°C, 1.08 V	65°C, 1.20 V	25°C, 1.32 V	25°C, 1.44 V
	FRR	FRR	FRR	FRR	FRR
12	85.12%; 90.11%	21.23%; 37.21%	1.04%; 4.95%	20.57%; 46.16%	48.95%; 83.48%
14	77.72%; 84.23%	13.69%; 25.98%	0.37%; 4.08%	12.78%; 34.63%	37.30%; 75.10%
16	69.35%; 77.89%	8.12%; 17.09%	0.14%; 3.52%	7.41%; 25.71%	26.97%; 66.32%
18	60.11%; 69.80%	4.68%; 10.78%	0.03%; 3.19%	4.12%; 17.08%	18.08%; 56.87%
20	50.64%; 61.17%	2.43%; 6.36%	0.01%; 2.89%	2.23%; 11.04%	11.53%; 46.36%
22	41.02%; 51.01%	1.29%; 3.93%	0.01%; 2.59%	1.13%; 7.06%	7.26%; 37.05%
24	32.08%; 43.10%	0.63%; 2.05%	0%; 2.33%	0.54%; 4.07%	4.21%; 29.38%
26	24.75%; 33.93%	0.23%; 1.27%	0%; 2.10%	0.28%; 2.58%	2.20%; 20.93%

The FRR from empirical evaluations and FRR statistical analyses based on Eq(9) are listed for comparison, where the format is (empirical); statistical).

5.3.3 Validation with a LAPUF

We use the k -sum ROPUF as a representative of the LAPUF to validate the TREVERSE-B.

LAPUF dataset description: Frequency measurements of all ROs of Virginia Tech’s ROPUF are leveraged to form k -sum ROPUF. We evaluated five k -sum ROPUFs; each of them is constructed in one FPGA board by using 128 ROs— $k = 64$. The frequency summation and consequent comparison are post-processed using MATLAB. Among five evaluated k -sum ROPUFs, the most noisy k -sum ROPUFs with worst-case BER of 14.53% occurred at (0.96 V, 25°C), while the (1.20 V, 25°C) acts as the nominal operating corner. For convenience, we will henceforth refer to the k -sum ROPUF as LAPUF.

Extraction of λ_1 and λ_2 from LAPUF model: The reliability confidence information of the LAPUF is *predicted* by the LAPUF model that serves as SimPUF. We use 10,000 challenges to extract λ_1 and λ_2 .

The reliability confidence of the response bit of the LAPUF is the frequency subtraction (difference) between the top and bottom RO rows. By predicting frequency differences given all response bits through the LAPUF model under the nominal operating condition and plotting all frequency differences, the standard variance is recognized as σ_{INTER} and the mean is the μ_{INTER} .

To extract σ_{INTRA} , the frequency differences given all response bits are *predicted* by the LAPUF model trained by CRPs evaluated under the nominal condition (1.20 V, 25°C) as a *reference*, then frequency differences for all the same response bits are predicted again by the LAPUF model trained with CRPs evaluated under a *differing* operating condition, e.g., (0.96 V, 25°C). The change between these two evaluations is calculated. By plotting 10,000 frequency changes, a distribution is obtained. Then its standard deviation is recognized as the σ_{INTRA} . Once the σ_{INTER} , μ_{INTER} and σ_{INTRA} are acquired, the λ_1 and λ_2 can be directly determined.

Results: Empirically and statistically evaluated FRR of the LAPUF are shown in Table 3. Instead of the empirical FRR always being smaller than the statistical FRR as is the case for the ROPUF in Table 2, they almost perfectly agree with each other for the LAPUF. Recall that the conservative statistical FRR for ROPUF is induced by the response bias

TABLE 3

FRR of the LAPUF under different operating conditions and m settings, where $k = 64$. Referenced operating condition (1.20 V, 25°C).

m	25°C, 0.96 V	25°C, 1.08 V	65°C, 1.20 V	25°C, 1.32 V	25°C, 1.44 V
	FRR	FRR	FRR	FRR	FRR
12	98.73%; 98.00%	59.59%; 56.87%	6.02%; 6.21%	44.31%; 39.21%	75.20%; 73.37%
14	97.55%; 96.37%	48.38%; 45.14%	2.60%; 3.72%	32.42%; 30.10%	65.82%; 62.74%
16	95.57%; 93.83%	36.98%; 34.97%	1.03%; 2.63%	22.73%; 20.50%	55.72%; 52.83%
18	93.16%; 90.37%	27.01%; 26.02%	0.51%; 2.08%	15.10%; 14.32%	45.56%; 42.71%
20	89.56%; 85.35%	19.06%; 17.37%	0.19%; 1.81%	9.33%; 8.42%	34.95%; 33.56%
22	84.79%; 80.29%	12.64%; 12.52%	0.05%; 1.62%	5.49%; 5.09%	26.21%; 24.52%
24	79.25%; 72.50%	8.17%; 7.57%	0.05%; 1.44%	3.07%; 2.89%	18.80%; 17.74%
26	72.50%; 66.00%	4.85%; 4.82%	0.02%; 1.29%	1.64%; 1.69%	13.14%; 12.28%

The FRR format is same with that of Table 2.

36.65% of the ROPUF, while the response bias of the investigated LAPUF is equal to 50.05%. Therefore, the statistical FRR accurately reflects the empirical FRR *even though the statistical FRR evaluation of the LAPUF is built upon learned LAPUF models*.

5.3.4 Summarize

Our extensive analysis of the ROPUF and LAPUF validate the derived FRR, which reflects the empirical FRR well. It is worth to note that the statistical FRR is a bit conservative evaluation of the empirical FRR when the PUF is with a moderate bias.

5.3.5 Remark

To accurately assess the FRR, two crucial parameters λ_1 and λ_2 (as function of σ_{INTER} , σ_{INTRA} , μ_{INTER} , with $\lambda_1 = \frac{\sigma_{\text{INTRA}}}{\sigma_{\text{INTER}}}$ and $\lambda_2 = \frac{\mu_{\text{INTER}}}{\sigma_{\text{INTER}}}$) are required. As we have experimentally showcased, determination of σ_{INTER} , σ_{INTRA} , μ_{INTER} is easy and only a one-time task to the server at the PUF provisioning phase. To be precise, it is just enrolling two SimPUFs given the same PUF but under two operating conditions—one under nominal operating condition, the other under (expected) worse-case operating corner.

6 AUTHENTICATION CAPABILITY EVALUATIONS

The previous section formalizes the FAR and FRR, and validates the accuracy of the FRR that is derived from an accurate PUF reliability model. In this section we analyze the authentication capability for both ROPUF and LAPUF.

From a practical perspective it is very important to have a small m because m stands for the computation overhead of the server. The smaller m , the less computation for the server to authenticate a single token. In this section, we present two simple, efficient and *compatible* methods to implement TREVERSE authentication in practice to achieve industry accepted false rejection rates.

6.1 d -Authentication

The first method is d -authentication. In one *authentication session*, the server issues d challenges $\{c_1, \dots, c_d\}$. The prover sequentially returns d outputs $\{\tilde{r}_1, \dots, \tilde{r}_d\}$. The server verifies the authenticity of each received output in sequential order. Authentication succeeds once a received output is accepted after which the server stops checking the rest. If *none* of the d received outputs can pass the authentication, then

this authentication session is rejected. By assuming each received output is independent, the FRR of d -authentication, FRR_d , is given as:

$$FRR_d = FRR^d \quad (10)$$

Detailed results of FRR_d of ROPUF and LAPUF are in the Appendix.

FAR_d is computed as:

$$FAR_d = d \times FAR. \quad (11)$$

We can see that d -authentication *linearly* increases FAR while *exponentially* minimizes FRR.

6.2 Multiple-Reference

The second method explores multiple reference responses to enhance the authentication capability. Overall, at the provisioning phase, multiple responses e_{ref} and their corresponding $conf_{ref}$ under discrete operating corners subject to the same challenges applied to the same PUF are enrolled. In other words, instead of enrolling one SimPUF under only one operating condition—nominal condition, multiple SimPUFs are enrolled under discrete operating corners.

Taking ROPUF as an example to ease understanding, during the enrollment phase, the frequencies of all ROs are measured under two operating corners: (25°C, 1.08 V) and (25°C, 1.32 V). As a consequence, the e_{ref_1} , e_{ref_2} and their corresponding $conf_{ref_1}$, $conf_{ref_2}$ are obtained, where ref_1 and ref_2 are operating corners of (25°C, 1.08 V) and (25°C, 1.32 V), respectively. During the authentication, for each received \tilde{r} , TREVERSE authentication is performed on \tilde{r} based on both e_{ref_1} , e_{ref_2} at the same time. If any one of two TREVERSE authentications passes— $\tilde{r} = r_{ref_1}$ or $\tilde{r} = r_{ref_2}$, the authentication succeeds. This helps decreasing the FRR significantly.

By assuming each referenced response is independent⁹ the FRR when multiple-reference is utilized, denoted as FRR_{mr} , is formalized as:

$$FRR_{mr} = \prod_{i=1}^M FRR_{ref_i} \quad (12)$$

with FRR_{ref_i} is the FRR when a single referenced operating corner is used for TREVERSE authentication. M is the number of referenced operating corners enrolled.

As for the FAR_{mr} , it only *linearly* increases in M :

$$FAR_{mr} = FAR \times M \quad (13)$$

6.3 Merging d -Authentication and Multiple-Reference

The above two augmented authentication methods are compatible with each other. They can be implemented together and the steps are detailed in Algorithm 2. Generally, if the TREVERSE fails by using a single output \tilde{r} from the prover, the server can ask the prover to refresh a new \tilde{r} according to the server issued new challenge c . The number of refreshment is preset to be no more than d . For each $\tilde{r}_i, i \in 1, \dots, d$,

⁹ Empirical results of FRR_{mr} of ROPUF and LAPUF in the Appendix show that this independence assumption is appropriate.

Algorithm 2 d -authentication and multiple-reference

```

1:  ▷ Server has enrolled multiple SimPUFs, with number
    of  $M$ , under  $M$  different operating conditions for the same
    PUF.
2:  procedure AugmentAuthenticate ( $M$  SimPUFs)
3:     $authState \leftarrow$  Fail
4:    for  $i = 1 : d$  do
5:      Send challenge  $c_i$  to prover and receive
       $\tilde{r}_i = \text{OWF}(\tilde{e}_i, n_i)$  from the prover
6:      for  $j = 1 : M$  do
7:        using SimPUF $_j$  to perform TREVERSE according
        to Algorithm 1
8:        if Success then
9:          return  $authState \leftarrow$  Success      ▷ Stop
        executing—escape from both the inner and out for loop
        end if
10:     end for
11:   end for
12: end procedure

```

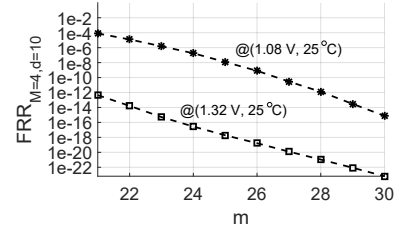


Fig. 8. The $FRR_{M,d}$ of ROPUF with ($M = 4, d = 10$ and $k = 110$). Four reference responses are from (0.96 V, 25°C), (1.20 V, 25°C), (1.20 V, 65°C) and (1.44 V, 25°C).

the server sequentially uses one of M enrolled SimPUFs—each SimPUF is enrolled under a different operating condition given the same PUF—to perform TREVERSE according to the algorithm 1. If it succeeds, then the server stops to i) use the rest SimPUFs to perform TREVERSE and ii) ask further \tilde{r} refreshments from the prover. Otherwise, the server continues to use the SimPUFs to perform TREVERSE and ask for further \tilde{r} refreshments. If after i) d times of \tilde{r} refreshments and ii) performing TREVERSE through all M SimPUFs for each \tilde{r} refreshment, the authentication is still not successful, then this authentication session fails.

When both methods are implemented together, the FRR and FAR are termed as $FRR_{M,d}$ and $FAR_{M,d}$ and expressed as:

$$FRR_{M,d} = \left(\prod_{i=1}^M FRR_{ref_i} \right)^d. \quad (14)$$

$$FAR_{M,d} = FAR \times M \times d. \quad (15)$$

M stands for the number of referenced responses and d is the number of authentication rounds used during one authentication session. FRR_{ref_i} is given by Eq(9) and FAR is given by Eq(2).

When an exhaustive trial and error approach is adopted, the maximum number of trials is equal to

$$N_{worst} = 2^m \times M \times d. \quad (16)$$

Both ROPUF and LAPUF are extensively tested when d -authentication and multiple-reference are employed together. The $FRR_{M,d}$ of ROPUF and LAPUF are detailed

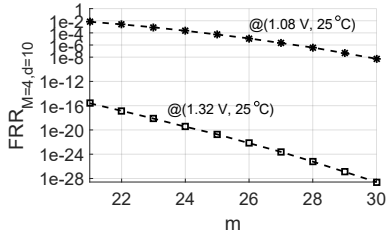


Fig. 9. The $FRR_{M,d}$ of LAPUF with ($M = 4$, $d = 10$ and $k = 110$). Four reference responses are from (0.96 V, 25°C), (1.20 V, 25°C), (1.20 V, 65°C) and (1.44 V, 25°C).

in Fig 8 and Table 9, respectively, where ($M = 4$, $d = 10$ and $k = 110$). The four reference responses are from (0.96 V, 25°C), (1.20 V, 25°C), (1.20 V, 65°C) and (1.44 V, 25°C)¹⁰. Under such setting, the worst case N_{worst} is around 2^{27} and 2^{29} for ROPUF to achieve $FRR_{M,d} < 10^{-3}$ and $FRR_{M,d} < 10^{-6}$, respectively. The N_{worst} is around 2^{29} and 2^{31} for LAPUF to achieve $FRR_{M,d} < 10^{-3}$ and $FRR_{M,d} < 10^{-6}$ because the LAPUF is more noisy than the ROPUF—14.53% worst ϵ of LAPUF versus 9.66% worst ϵ of ROPUF.

7 COMPARISON AND DISCUSSION

7.1 Comparison

Table 4 includes six finalists out of 21 PUF-based authentication protocols examined by Delvaux (Chapter 5.4) [12]. Whereas protocols that i) do not offer *any* resistance to both noise and machine learning attacks, ii) are vulnerable to conventional protocol attacks and iii) are not suitable for implementation purposes, are excluded. We notice that Slender PUF [23] and Lockdown [31] can resist conventional modeling attacks e.g., SVM, logistic regression, but are vulnerable to other forms of modeling attacks [37], [59]. Delvaux [16] recently reviewed the other 5 up-to-date PUF-based authentication protocols, which we also include. We compare TREVERSE with the PUF based authentications listed in Table 4.

From Table 4, we can see without OWF, it is extremely hard, if not impossible, to resist modeling attacks (e.g., the entries from Slender to LHS-PUF) unless the lockdown technique (detailed in Section 8.3) is deployed to explicitly limit the CRPs available by the adversary. Without adequate CRP for training, an accurate model is infeasible to be learned, thus, preventing modeling attacks. However, lockdown inevitably sacrifices practicality of the PUF authentication because only a limited number of authentications, e.g., 1000 can be securely issued. Afterwards, the PUF integrated token has to be disposed to maintain security.

When OWF is used (e.g., the entries from Sadeghi to Controlled), ECC logic and associated helper data are always required. Unfortunately, the ECC logic is very expensive, see experimental validation in Section 7.2.1. Moreover, the helper data has to be carefully handled to avoid information leakage and helper data manipulation attacks [60],

¹⁰. We are limited by fine-grained reference in the tested public dataset. Once more fine-grained reference are employed in practice, the m will be greatly decreased given the fixed FRR. Herein, we constrain our tests on the public dataset.

TABLE 4
PUF based Authentication Comparison

	token authenticity	server authenticity	TRNG	ECC logic	OWF	Authentication rounds	PUF independent	Modeling resistance	Comparable to Class. Authen. ^a
Slender [23]	✓	×	✓	×	×	8	×	×	N/A
Noise bifur. [22]	✓	×	✓	×	×	8	×	×	N/A
PolyPUF [62]	✓	×	✓	×	×	8	×	×	N/A
OB-PUF [24]	✓	×	✓	×	×	8	×	×	N/A
RPUF [63]	✓	×	✓	×	×	8	×	×	N/A
LHS-PUF [64]	✓	×	✓	×	×	8	×	×	N/A
Lockdown I [31]	✓	✓	×	×	×	8	✓	✓	N/A
Lockdown II [31]	✓	✓	✓	×	×	8	✓	✓	N/A
Sadeghi [65]	✓	×	✓	✓	✓	8	✓	✓	×
Rever. FE II [47]	✓	×	✓	✓	✓	8	✓	✓	×
Controlled [50]	✓	×	×	✓	✓	8	×	×	×
PUF-FSM [66]	✓	✓	×	×	✓	8	×	×	×
TREVERSE-A	✓	×	×	×	✓	8	×	×	✓
TREVERSE-B	✓	✓	✓	×	✓	8	✓	✓	✓

^a Is the PUF authentication instantiation on the token comparable to the classical key based entity/client dynamic authentication as depicted in Fig. 22. In this context, to be fair, we only compare with those PUF key based authentication as all of them require OWF.

[61]. Regarding to the PUF-FSM that does remove the ECC logic, it is, however, still vulnerable to modeling attack [16] because of the response reliability information (highly reliable responses) is leaked.

Overall, we can see that the on-chip TRNG is a common building block in the PUF based authentication. Indeed, without it, mutual authentication realization is impossible.

According to Delvaux's aftermath in [16]: "A fairly conservative approach to craft a PUF-based authentication protocol is to convert a noisy response into a stable secret key and then use a keyed cryptographic algorithm to perform the authentication". Our TREVERSE, to a large extent, falls into the keyed cryptographic approach but we counter-intuitively remove the requirement of expensive ECC logic and the worries on securely handling of the helper data. In comparison with the lockdown, we eschew the fetter of limited authentications by exploiting a OWF that is still lightweight and further significantly enhances the security.

Overall, TREVERSE, for the first time, ultimately enables a generic PUF based authentication mechanism to be comparable with the classical digital key based dynamic authentication as shown in Fig. 2 since the noisy PUF response is oblivious to the prover and is treated as a digital key. We would like to remind that whenever mutual authentication is built upon a digital key, the on-chip TRNG is also in need in order to provide token side freshness.

7.2 Discussion

7.2.1 Server and Prover Overhead

We evaluate the overhead of the TREVERSE from the server and prover side, respectively.

Server Overhead: The server setting is detailed in Appendix D. Generally, the time T_s required for the server

to complete one TREVERSE authentication session can be estimated by:

$$T_s = N_{\text{worst}} \times k \times \frac{1}{8} \times \frac{1}{\text{Hash}_{\text{speed}}} \times \frac{1}{N_{\text{GPUcore}}} \times \frac{1}{N_{\text{CPUcore}}} \quad (17)$$

where N_{worst} the number of trials that the server needs to perform in the worst case, k the length of response e , and N_{GPUcore} and N_{CPUcore} the number of GPU cores and the CPU cores, respectively, equipped by the server. The Fig. 10 illustrates the T_s as a function of N_{worst} given the settings of $k = 128$, $\text{Hash}_{\text{speed}} = 648$ MiBps, number of GPU cores of 1920, and number of CPU core of one and four, respectively. As an example, to tolerate a 14.53% BER of the LAPUF while maintaining the $\text{FRR} < 10^{-6}$, 2^{31} trials in worst case is required by the server, which only needs 28 ms and 7 ms when employing a CPU with a single core and four cores, respectively.

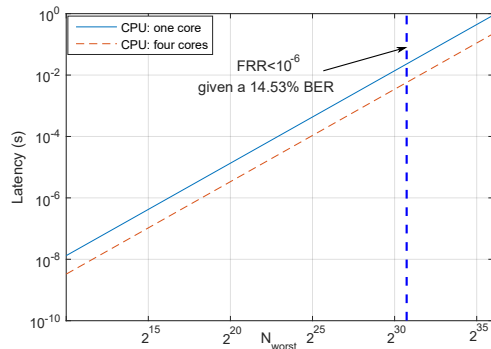


Fig. 10. Estimated server time latency T_s as a function of the worst-case trial numbers N_{worst} under a common personal computer computational power settings, detailed in Appendix D.

Prover ECC vs TREVERSE Overhead: We choose a MSP430FR5969 microcontroller and BCH code as error correction code (ECC) to evaluate the prover overhead in terms of clock cycles, detailed prover settings and descriptions are in Appendix .E. In general, the ECC enabled authentication builds upon either through reverse fuzzy extractor (RFE) that employs the ECC encoding on-chip or fuzzy extractor (FE) that employs the ECC decoding on-chip. Based on the settings detailed in Appendix .E. the time latency for the RFE in the prover side (MSP430FR5969 microcontroller) costs 2.55 s according to the Table 17 if it is required to achieve a 10^{-6} FRR given a BER of 14.53%. Please note that for such resource-constraint provers, the time latency of implementing the FE that employs ECC decoding tends to be unacceptable, e.g., could take more than 100 s.

According to the evaluation results in Section 6.3, the prover may run $d = 10$ times successively in the worst case under the d -authentication to lower the $\text{FRR} < 10^{-6}$ tolerating the worst-case BER of 14.53% of the LAPUF. Therefore, the clock overhead for the prover in the worst case is performing $d = 10$ times hash operations, which cost 1,047,230 clock cycles, taking about 1 s. We can see that the TREVERSE greatly outperforms the ECC based authentication—reducing by 60%—even when the lightweight RFE [67] rather the common FE is employed.

Besides the overhead, the TREVERSE inherently removes potential security vulnerabilities induced from ECC and associated helper data as detailed in the next Section 7.2.2.

In fact, the server can choose to increase m , thus, number of trials, to further decrease the d needed in the prover side, which could reduce the worst-case overhead (clock cycles) of the prover. In addition, we can see that in practice, the latency bottleneck seems usually located in the prover side rather the server side. Therefore, it is desirable to reduce the prover side overhead as much as possible considering the fact that the server side can be powerful and flexibly configured, which is what the TREVERSE is motivated and designed for.

7.2.2 Security

In comparison with PUF authentication without OWF, our TREVERSE is straight forwardly secure against modeling attacks because of the hardness of inverting the OWF. In comparison with PUF authentication with OWF which requires ECC logic and thus helper data, our TREVERSE is also more secure because there is no ECC and associated helper data involved.

Helper data manipulation (HDM) attacks [60], [61] have demonstrated various error correction code and the decoding strategy of the code’s implementation are vulnerable. A generic countermeasure against recent Becker’s HDM attacks does not yet exist, appears to be an open challenge, especially to the robust fuzzy extractor [61]. In this context, we are only aware, to date, that the linear BCH code based syndrome decoding is proven to be immune to the HDM attack ¹¹. Therefore, this is the reason why we opt for evaluating the ECC overhead based on the BCH code based syndrome decoding in Section 7.2.1.

Since TREVERSE requires no ECC, consequently, no helper data, helper data manipulation attacks [60], [61] are inherently eschewed.

7.2.3 Generic

Firstly, the TREVERSE authentication is generic to all PUF types as long as the PUF has its corresponding SimPUF. Secondly, the validated two simple yet efficient and complementary augmentation methods— d -authentication and multiple-reference—to enhance TREVERSE authentication capability are also independent on PUF types.

7.2.4 Server-Aided

The TREVERSE fully takes advantage of a resource-rich server. It is the server enrolling and storing the SimPUF during the enrollment, then grading the PUF response reliability confidence, and the server carries out the trials and checks during the authentication phase. In addition, when multiple referenced response technique is used to significantly augment the authentication capability, the server takes all the overhead without bringing any overhead to the token even if more referenced responses are used.

¹¹. A detailed discussion and a proof that syndrome based decoding is immune from the HDM attacks presented by Becker can be found in Section 6.1 of the article in [61]

7.2.5 Countering Aging or Fault Induced Errors

TREVERSE inherently eschews security concerns associated with ECC associated helper data. However, if there are drastic variations in the PUF response specific reliability model due to ageing, it is possible for TREVERSE to result in increased key failure rates.

Notably, ageing is PUF design specific, there exists methods of countering aging related behaviour changes of a given PUF design—see [68] for SRAM PUFs and see [69] for ROPUFs. Therefore, we believe these existing counter measures can be adopted to combat ageing related degradation on TREVERSE performance.

Nonetheless, by slightly modifying the trial-and-error method used in TREVERSE, we can handle the rare errors that occur in the most reliable bits. We refer to this mechanism as the detection-update trial-and-error, where the detection-update concept is similar to [70]. As illustrated in Fig. 11, we suppose that the server has already sorted the k response bits according to reliability—the e_1 with the highest reliability and e_k with the lowest reliability. Besides trying all error patterns for all the m unreliable bits, the server can periodically, considering the rate of aging of the hardware, or when abnormally high rejection rates are observed, iteratively flip one or two bits within $k-m$ reliable bits. If any bits within this $k-m$ reliable bits are found to be flipped on the PUF integrated device, the server can detect it through iterative trial and error checks. Consequently, the server can update the bit value on the server side within this $k-m$ reliable bits to compensate for aging induced errors on the PUF device.

In this context, the number of trials performed by the server becomes $\binom{k-m}{n_{ag}} \times 2^m$ with n_{ag} the number of errors induced by *aging or unexpected faults*. Notably, the value n_{ag} will be very small, since the server can pick a short period, e.g. once within a one month, to conduct the update to ensure changes due to any ageing affects are minimal. This periodical detection-update trial-and-error will bring an extra $\binom{k-m}{n_{ag}}$ multiple to the trials in comparison with the original exhaustive search over the m unreliable bits. However, it is worth noting that such a detection-update trial-and-error is not needed for normal authentication sessions but, rather, performed periodically. Moreover, when performing detection-update trial-and-error, the server can first reduce m to decrease the trials because we know that 2^m trials are only needed in the worst case. For example, given $k = 110$, the server can set $m = 27$ resulting in 2^{27} trials in the worst case for trial-and-error, for the detection-update trial-and-error the server can reduce m to be 22 and set $n_{ag} = 1$, giving $\binom{88}{1} \times 2^{22} < 2^{29}$ trials in the worst case.

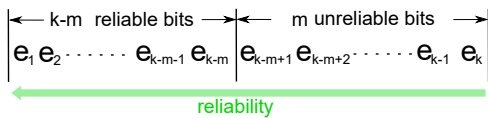


Fig. 11. Detection-update trial-and-error performed periodically or when abnormally increased rejection rate occurs as a general approach to counter aging or fault induced flipped bits in reliable bits.

This detection-update and trial-and-error mechanism brings extra management overhead to the server. However,

the errors resulting from aging or faults are expected to be infrequent. For example, Maes *et al.* [71] reported a maximum unreliability increase of 3.9% from 4.5 years ageing for ROPUFs, here, approximately 1 bit is flipped out of 128 bits per year due to aging. Thus, the extra management overhead is slight. In addition, TREVERSE is designed to utilize a resource-rich server that can be flexibly configured and is computationally powerful; therefore, such a light overhead increase is acceptable in order to achieve a lightweight and secure implementation on the resource-constraint device.

Overall, we have provided methods for addressing ageing at the protocol level and the device level, accounting for ageing by considering an adaptation of the SimPUF is both a challenging and interesting direction for our future work. We believe such a method can allow TREVERSE to function without the slight increase in sever overhead to deal with ageing or the use of device level methods to combat ageing related influences on PUF response.

8 RELATED WORK

PUF based authentication mechanisms must directly deal with noise inherent to the source of entropy used for deriving keys. The solutions to address a noisy PUF response broadly fall into three approaches: i) PUF re-engineering to enhancing response reliability (see Section 8.1); ii) Reconciling response errors (See Section 8.2); iii) Response similarity measures (see Section 8.3). The method selected for dealing with noisy responses dictates the authentication protocol, cost of implementation on the token, the range of PUF primitives that can be used with the authentication protocol as well the security and practicality of the mechanism. We discuss related work based on the above methods.

TREVERSE explicitly employs the bit specific nature of PUF responses as a trapdoor. A recent and closely related study in [27] employed a response reconciliation method requiring on-chip based measurements of bit specific reliability, which is discussed in Section 8.2.

8.1 PUF re-engineering: enhancing response reliability

The aim of PUF re-engineering is i) to design intrinsic reliable PUF or ii) special PUFs that facilitate winnowing high reliable responses.

A digital PUF [17]–[19] is typically an intrinsic reliable PUF to achieve a noisy free PUF. In general, a digital PUF response is not susceptible to environmental parameter fluctuations. As an example, intentional design defects can be utilized to induce faults in a digital circuit, hence dramatically impacting its logic functionality. Instead of process variations, these faults can be used as a ‘fingerprint’ for a digital PUF [18], [19]. However, a digital PUF always requires dedicated design steps such as layout consideration [19] and even special fabrication steps such as hot carrier injection [17], time-dependent dielectric breakdown [72]. Recent works also utilize properties of emerging nano elements such as memristor [73] and phase change memory [74] to realize intrinsic reliable PUFs. However, such emerging PUF constructions are not likely to be deployed in practice in the near future.

In [20], Bhargava *et al.* construct a so called sense amplifier PUF (SAPUF), which uses each sense amplifier (SA) cell

to generate one response—architecture is alike SRAM PUF but replaces each SRAM cell with SA cell. In this SAPUF, using built-in self-test, the reliability of the PUF response can be determined by the magnitude of the unavoidable offset voltage of a SA introduced from the manufacturing randomness. The larger the offset voltage, the more reliable the SAPUF response. In [20], a bitmap (location mask) of reliable responses are employed as helper data only readable but not writable by an attacker; consequently, the helper data needs to be stored on-chip.

Overall, the PUF re-engineering is constructing a special PUF rather than a general approach that tackles reliability issues of existentially easy to fabricate popular silicon PUFs. While TREVERSE is a general framework for any PUF type with a simulatable PUF.

8.2 Reconciling Response Errors

In literature, stabilizing response errors usually targets the PUF based key generation application—works targeting authentication may choose [8] simple error correction code, mainly for weak PUFs with limited CRP space. The PUF key generator to derive a reliable key from noisy PUF responses usually comprises two components: secure sketch and entropy accumulator. Both together are usually referred to as a fuzzy extractor [60], [75]. The secure sketch is responsible for reconciling noisy responses, which has two prevalent constructions: code-offset and syndrome based [60]. Regardless of the specific construction, the secure sketch is a pair of randomized procedures: the sketching procedure takes a response r as an input, then computes the enrolled key and the helper data; the recovery procedure takes both the helper data and a reevaluated response r' to reconstruct the enrolled key. The set of responses might not be ideally uniformly distributed, thereby, the entropy accumulator compresses the input response into a cryptographic key with uniform distribution relying on a random oracle, OWF.

As experimentally validated in Section 7.2.1, although the OWF implementation (entropy accumulator in fuzzy extractor) in practice can be lightweight, the ECC logic (secure sketch in the fuzzy extractor) is usually very expensive. Therefore, the fuzzy extractor is hard to be directly mounted to secure resource tight IoT devices. In addition, the helper data that is needed when using a fuzzy extractor has to be carefully handled to eliminate attacks introduced by itself.

Our TREVERSE resolves the above deficiencies as the ECC logic and helper data are no longer needed.

Reverse Fuzzy Extractor: In general, sketching and recovery procedures are realized via ECC encoding and decoding, respectively. As the ECC decoding is computationally more intensive than encoding, one can embed the ECC encoding logic (ie. a computationally lighter sketching procedure) in the resource-restricted PUF. The computationally harder decoding logic is performed by a resource-rich server. This arrangement is called a reverse fuzzy extractor [67]. The reverse fuzzy extractor exploits the server to do intensive computation.

We use the ‘reverse’ term to *only* refer to the exploitation of a resource-rich server to perform authentications. Neither ECC decoder nor encoder exist in TREVERSE.

Our TREVERSE removes the ECC logic, therefore, it is lightweight. The TREVERSE also removes helper data,

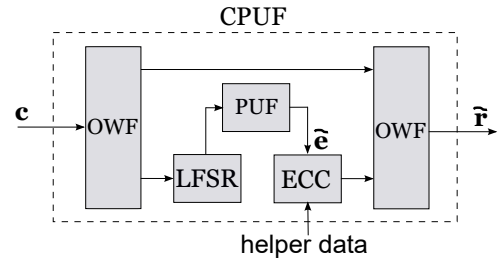


Fig. 12. Generalized controlled PUF (CPUF) construction. Noting in practice, only one OWF logic implementation is required to save area overhead, while this OWF is sequentially used twice.

therefore, it has better security because potential attacks such as helper data manipulation attack [15], [60], [61] and reliability-based modeling attacks [37], [76] are inherently avoided.

Fuzzy Extractor with trapdoor: Herder *et al.* [27] propose the computationally-secure fuzzy extractor to extract cryptographic keys from the PUF. In this context, the response reliability confidence information is, for the first time, treated as a trapdoor to build up a stateless key generator, while previous works do take bit-specific reliability into consideration to improve the efficiency of PUF key derivation but public such information. In other words, the response reliability information now is never exposed but measured internally within the PUF key generator on demand—discarded after internal usage. In this context, the ROPUF is chosen for experimentally validations. Because the ROPUF’s response reliability confidence that can be directly acquired via subtracting frequencies of two ROs meets with the trapdoor requirement. However, for most PUF constructions the response reliability confidence is hard to be directly and easily measured on-chip. For instance, the APUF’s response reliability is not measurable on-chip unless using expensive peripheral circuits. Therefore, the stateless key generator exploiting the trapdoor reliability information is not, or at least difficult, applicable to other PUF structures.

Firstly, the TREVERSE does not require the token to measure the response reliability on-chip, which is suitable for a wide range of PUF types including LAPUFs, ROPUFs, and SRAM PUFs—as long as the PUF has its corresponding SimPUF. Secondly, in [27], the token has to take all the computation burden to reconstruct a stateless key that is targeted for key generation. Lightweight appears not the concern. Conversely, TREVERSE is the first to utilize the bit-specific reliability as trapdoor to realize lightweight and secure authentication by moving as much as computation from the token to the server.

8.3 Similarity Measures

For strong PUF authentication, the server compares the received response vector with its enrolled response vector given the same challenge. Based on the similarity, specifically, Hamming distance (HD) that majority work relies on due to its simplicity—there are other similarity metrics such as using fault tolerant ring weight scheme [77], between the received and enrolled response, the server accepts the authenticity of the prover on the condition that the HD is lower than a threshold, otherwise, rejects. To be specific,

such HD based authentication is only suitable for the strong PUF with a very large CRP (challenge) space to prevent fully CRP characterization within e.g., years. Notably, the practical HD-based lightweight authentication is always built upon the APUF or its variants such as XOR-APUF [32], Slender PUF [23], obfuscated APUF [22], [24]. Unfortunately, though might be lightweight, it has been shown that the security of the HD based authentication is very difficult to be guaranteed in presence of modeling attacks. According to recent survey on HD-based authentication [32], [37], [38] in Delvaux thesis in 2017 [12], all these HD-based authentication are broken under modeling attacks except the lockdown PUF.

The lockdown PUF restricts the maximum number of LAPUF CRPs that can be acquired by an adversary [31]. This is achieved by an explicit CRP release. Generally, the token and the server together determine challenges presented to the LAPUF. Responses are divided into two subparts, the first subpart needs to be firstly provided by the server. The later subpart is visible only when the first subpart response sent from the server is close enough to that generated by the token. Thus, an adversary is unable to obtain new CRP materials without authorization from the server. Once a number of CRPs have been issued, the token has to be disposed and never used again, which results into a usage trade-off of limited authentication rounds, e.g., typically 1000 times [31]. Unlike other HD-based authentications, the lockdown, in essence, *not intends to invent an architecture to increase the complexity of modeling attacks by the adversary*. In the other way round, it limits the ability of obtaining an adequate number of CRPs for training by the adversary to prevent modeling attacks.

We notice one PUF authentication based on HD comparison occasionally uses the ‘trial and error’ inexplicitly [78]. Therefore, we briefly introduce it to show their trial and error is used in a totally different manner [78]. This design has been shown impractical and insecure, we refer in-depth analysis to [12] (Chapter 5.3.4). Generally, the token implementation has two strong PUFs, specifically, APUFs: an inner APUF and an outer APUF. The server learns models of both APUFs during enrollment phase in order to emulate response given a random challenge. The inner PUF becomes not accessible once it is deployed in field. There is an initial state s with length n of inner APUF that acts as a challenge seed. Noting s in [78] requires a secure NVM, which undermines the PUF value [12]. When authentication starts, this s is expanded into n subchallenges to generate a concatenated response e_1 . This e_1 is then XORed with the challenge c issued by the server and then is applied to the outer APUF to produce response e_2 sent to server for authentication. Meanwhile, the s is updated by e_1 . In [78], it is claimed that the e_1 can be always stable, e.g., by using major voting technique, and is therefore the same as the \bar{e}_1 emulated by the server. In the worst case, it is assumed that there is 1 out of n errors. This error will desynchronize the authentication. In this context, *the server iteratively flips each bit of \bar{e}_1 to try authentication for synchronization*. To this end, we can see this occasional trial and error usage is totally different from ours.

8.4 Summary

TREVERSE distinguishes from the above approaches by constructively exploiting bit-specific reliability to tackle noisy PUF responses through a trial-and-error approach at the server.

9 CONCLUSION AND FUTURE WORK

The developed TREVERSE fully leverages a computational resource-rich server to ensure a (mutual) lightweight token realization. The TREVERSE allows the prover to directly processes noisy PUF responses via OWF, it ultimately discards expensive ECC logic, thus, removing the necessity of the helper data that is exploitable by an adversary. Through implementing d -authentication and multiple-reference that complement each other to exponentially enhance the authentication capability, we are able to reduce the FRR to be less than 10^{-6} by tolerating BER up to 9.66% and 14.53% for ROPUF and LAPUF while maintaining trial computations being practically acceptable to the server, even a personal computer.

i) The current TREVERSE utilizes an exhaustive search over least reliable bits, which is not the best optimization. Future work can investigate other efficient search approach to further improve the authentication efficiency. ii) One limitation of the current experimental evaluation is that the aging effect is not included. We leave this as a future work. We believe that the aging effect can be easily addressed, especially by utilizing more references via the multiple-reference technique. iii) Another future work can investigate the TREVERSE instantiation through the AISC APUF instance that is also a typical representative of the LAPUF. iv) It is also valuable to test a TREVERSE instantiation using intrinsic SRAM PUFs. In this context, the key is to expedite the bit reliability information enrollment, ideally by evading the exhaustively repeated physical measurements.

10 ACKNOWLEDGMENT

We thank Yang Su for evaluating part of results in Table 16.

REFERENCES

- [1] B. Gassend, D. Clarke, M. Van Dijk, and S. Devadas, “Silicon physical random functions,” in *CCS*, 2002, pp. 148–160.
- [2] G. E. Suh and S. Devadas, “Physical unclonable functions for device authentication and secret key generation,” in *DAC*, 2007, pp. 9–14.
- [3] L. Zhang, C. Wang, W. Liu, M. O’Neill, and F. Lombardi, “XOR gate based low-cost configurable RO PUF,” in *ISCAS*. IEEE, 2017, pp. 1–4.
- [4] M. T. Rahman, F. Rahman, D. Forte, and M. Tehranipoor, “An aging-resistant RO-PUF for reliable key generation,” *IEEE Trans. Emerg. Topics Comput.*, vol. 4, no. 3, pp. 335–348, 2016.
- [5] D. E. Holcomb, W. P. Bursleson, and K. Fu, “Initial SRAM state as a fingerprint and source of true random numbers for RFID tags,” in *Proceedings of the Conference on RFID Security*, 2007.
- [6] Y. Cao, L. Zhang, C.-H. Chang, and S. Chen, “A low-power hybrid RO PUF with improved thermal stability for lightweight applications,” *IEEE Trans. Comput.-Aided Design Integr. Circuits Syst.*, vol. 34, no. 7, pp. 1143–1147, 2015.
- [7] J. S. Kim, M. Patel, H. Hassan, and O. Mutlu, “The DRAM latency PUF: Quickly evaluating physical unclonable functions by exploiting the latency-reliability tradeoff in modern commodity dram devices,” in *HPCA*. IEEE, 2018, pp. 194–207.

- [8] S. Sutar, A. Raha, D. Kulkarni, R. Shorey, J. Tew, and V. Raghunathan, "D-PUF: An intrinsically reconfigurable DRAM PUF for device authentication and random number generation," *ACM Transactions on Embedded Computing Systems (TECS)*, vol. 17, no. 1, p. 17, 2018.
- [9] S. Sutar, A. Raha, and V. Raghunathan, "Memory-based combination pufs for device authentication in embedded systems," *IEEE Trans. Multi-Scale Comput. Syst.*, vol. 4, no. 4, pp. 793–810, 2018.
- [10] Y. Gao, D. C. Ranasinghe, S. F. Al-Sarawi, O. Kavehei, and D. Abbott, "Emerging physical unclonable functions with nanotechnology," *IEEE Access*, vol. 4, pp. 61–80, 2016.
- [11] C. Herder, M.-D. Yu, F. Koushanfar, and S. Devadas, "Physical unclonable functions and applications: A tutorial," *Proc. IEEE*, vol. 102, pp. 1126–1141, 2014.
- [12] J. Delvaux, "Security analysis of PUF-based key generation and entity authentication," Ph.D. dissertation, Shanghai Jiao Tong University, China, 2017.
- [13] O. Günlü and G. Kramer, "Privacy, secrecy, and storage with multiple noisy measurements of identifiers," *IEEE Trans. Inf. Forensics Security*, vol. 13, no. 11, pp. 2872–2883, 2018.
- [14] M.-D. M. Yu and S. Devadas, "Pervasive, dynamic authentication of physical items," *Communications of the ACM*, vol. 60, no. 4, pp. 32–39, 2017.
- [15] J. Delvaux, R. Peeters, D. Gu, and I. Verbauwhede, "A survey on lightweight entity authentication with strong pufs," *ACM Computing Surveys (CSUR)*, vol. 48, no. 2, p. 26, 2015.
- [16] J. Delvaux, "Machine-learning attacks on PolyPUFs, OB-PUFs, RPUFs, LHS-PUFs, and PUFSLMs," *IEEE Trans. Inf. Forensics Security*, vol. 14, no. 8, pp. 2043–2058, 2019.
- [17] M. Bhargava and K. Mai, "A high reliability PUF using hot carrier injection based response reinforcement," in *CHES*. Springer, 2013, pp. 90–106.
- [18] T. Xu and M. Potkonjak, "Digital PUF using intentional faults," in *IEEE Int. Symp. Quality Electronic Design*, 2015, pp. 448–451.
- [19] J. Miao, M. Li, S. Roy, and B. Yu, "LRR-DPUF: Learning resilient and reliable digital physical unclonable function," in *ICCAD*, 2016, pp. 1–8.
- [20] M. Bhargava and K. Mai, "An efficient reliable PUF-based cryptographic key generator in 65nm CMOS," in *DATE*, 2014, p. 70.
- [21] R. Maes, V. van der Leest, E. van der Sluis, and F. Willems, "Secure key generation from biased PUFs: extended version," *Journal of Cryptographic Engineering*, vol. 6, no. 2, pp. 121–137, 2016.
- [22] M.-D. Yu, D. M'Raihi, I. Verbauwhede, and S. Devadas, "A noise bifurcation architecture for linear additive physical functions," in *HOST*, 2014, pp. 124–129.
- [23] M. Rostami, M. Majzoobi, F. Koushanfar, D. S. Wallach, and S. Devadas, "Robust and reverse-engineering resilient PUF authentication and key-exchange by substrng matching," *IEEE Trans. Emerg. Topics Comput.*, vol. 2, no. 1, pp. 37–49, 2014.
- [24] Y. Gao, G. Li, H. Ma, S. F. Al-Sarawi, O. Kavehei, D. Abbott, and D. C. Ranasinghe, "Obfuscated challenge-response: A secure lightweight authentication mechanism for PUF-based pervasive devices," in *Percom Workshops*, 2016, pp. 1–6.
- [25] R. Maes, P. Tuyls, and I. Verbauwhede, "A soft decision helper data algorithm for SRAM PUFs," in *IEEE Int. Symp. Information Theory*. IEEE, 2009, pp. 2101–2105.
- [26] R. Maes, "An accurate probabilistic reliability model for silicon PUFs," in *CHES*, 2013, pp. 73–89.
- [27] C. Herder, L. Ren, M. van Dijk, M.-D. M. Yu, and S. Devadas, "Trapdoor computational fuzzy extractors and stateless cryptographically-secure physical unclonable functions," *IEEE Trans. Dependable Secure Comput.*, vol. 14, no. 1, pp. 65–82, 2017.
- [28] Y. Gao, S. F. Al-Sarawi, and D. Abbott, "Physical unclonable functions," *Nature Electronics*, vol. 3, no. 2, pp. 81–91, 2020.
- [29] A. Maiti, J. Casarona, L. McHale, and P. Schaumont, "A large scale characterization of RO-PUF," in *HOST*, 2010, pp. 94–99.
- [30] U. Ruhrmair and M. Van Dijk, "PUFs in security protocols: Attack models and security evaluations," in *IEEE Symp. Security and Privacy*, 2013, pp. 286–300.
- [31] M.-D. Yu, M. Hiller, J. Delvaux, R. Sowell, S. Devadas, and I. Verbauwhede, "A lockdown technique to prevent machine learning on PUFs for lightweight authentication," *IEEE Trans. Multi-Scale Comput. Syst.*, vol. 2, no. 3, pp. 146–159, 2016.
- [32] U. Ruhrmair, J. Solter, F. Sehnke, X. Xu, A. Mahmoud, V. Stoyanova, G. Dror, J. Schmidhuber, W. Burleson, and S. Devadas, "PUF modeling attacks on simulated and silicon data," *IEEE Trans. Inf. Forensics Security*, vol. 8, no. 11, pp. 1876–1891, 2013.
- [33] M.-D. Yu, D. M'Raihi, R. Sowell, and S. Devadas, "Lightweight and secure PUF key storage using limits of machine learning," in *CHES*. Springer, 2011, pp. 358–373.
- [34] M.-D. Yu, R. Sowell, A. Singh, D. M'Raihi, and S. Devadas, "Performance metrics and empirical results of a PUF cryptographic key generation ASIC," in *HOST*. IEEE, 2012, pp. 108–115.
- [35] D. Lim, "Extracting secret keys from integrated circuits," Master's thesis, Massachusetts Institute of Technology, 2004.
- [36] U. Ruhrmair, F. Sehnke, J. Sölter, G. Dror, S. Devadas, and J. Schmidhuber, "Modeling attacks on physical unclonable functions," in *CCS*, 2010, pp. 237–249.
- [37] G. T. Becker, "On the pitfalls of using Arbiter-PUFs as building blocks," *IEEE Trans. Comput.-Aided Design Integr. Circuits Syst.*, vol. 34, no. 8, pp. 1295–1307, 2015.
- [38] G. T. Becker, "The gap between promise and reality: On the insecurity of XOR arbiter PUFs," in *CHES*, 2015, pp. 535–555.
- [39] X. Xu, W. Burleson, and D. E. Holcomb, "Using statistical models to improve the reliability of delay-based PUFs," in *IEEE Computer Society Annual Symp. VLSI*. IEEE, 2016, pp. 547–552.
- [40] M.-D. Yu and S. Devadas, "Secure and robust error correction for physical unclonable functions," *IEEE Design & Test of Computers*, vol. 27, no. 1, pp. 48–65, 2010.
- [41] R. Maes, P. Tuyls, and I. Verbauwhede, "Low-overhead implementation of a soft decision helper data algorithm for SRAM PUFs," in *CHES*. Springer, 2009, pp. 332–347.
- [42] D. C. Ranasinghe, D. Lim, S. Devadas, D. Abbott, and P. H. Cole, "Random numbers from metastability and thermal noise," *Electronics Letters*, vol. 41, no. 16, p. 1, 2005.
- [43] Holcomb, Daniel E, W. P. Burleson, and K. Fu, "Power-up SRAM state as an identifying fingerprint and source of true random numbers," *IEEE Trans. Comput.*, vol. 58, no. 9, pp. 1198–1210, 2009.
- [44] V. van der Leest, E. van der Sluis, G.-J. Schrijen, P. Tuyls, and H. Handschuh, "Efficient implementation of true random number generator based on sram pufs," in *Cryptography and Security: From Theory to Applications*. Springer, 2012, pp. 300–318.
- [45] Y. Wang, W.-k. Yu, S. Wu, G. Malysa, G. E. Suh, and E. C. Kan, "Flash memory for ubiquitous hardware security functions: True random number generation and device fingerprints," in *IEEE Symp. Security and Privacy*. IEEE, 2012, pp. 33–47.
- [46] G. Zheng, Y. Lyu, and D. Wang, "True random number generator based on ring oscillator PUFs," in *Proc. 2nd Int. Conf. Multimedia Systems and Signal Processing*. ACM, 2017, pp. 1–5.
- [47] R. Maes, "Physically unclonable functions: Properties," in *Physically Unclonable Functions*. Springer, 2013, pp. 49–80.
- [48] D. P. Sahoo, D. Mukhopadhyay, R. S. Chakraborty, and P. H. Nguyen, "A multiplexer-based arbiter PUF composition with enhanced reliability and security," *IEEE Trans. Comput.*, vol. 67, no. 3, pp. 403–417, 2017.
- [49] P. H. Nguyen, D. P. Sahoo, C. Jin, K. Mahmood, U. Ruhrmair, and M. van Dijk, "The interpose PUF: Secure PUF design against state-of-the-art machine learning attacks," *IACR Transactions on Cryptographic Hardware and Embedded Systems*, pp. 243–290, 2019.
- [50] B. Gassend, D. Clarke, M. Van Dijk, and S. Devadas, "Controlled physical random functions," in *ACSAC*. IEEE, 2002, pp. 149–160.
- [51] B. Gassend, M. V. Dijk, D. Clarke, E. Torlak, S. Devadas, and P. Tuyls, "Controlled physical random functions and applications," *ACM Transactions on Information and System Security (TISSEC)*, vol. 10, no. 4, p. 3, 2008.
- [52] P. Tuyls, G.-J. Schrijen, B. Škorić, J. Van Geloven, N. Verhaegh, and R. Wolters, "Read-proof hardware from protective coatings," in *CHES*. Springer, 2006, pp. 369–383.
- [53] V. Immler, J. Obermaier, M. König, M. Hiller, and G. Sig, "B-TREPID: Batteryless tamper-resistant envelope with a PUF and integrity detection," in *HOST*. IEEE, 2018, pp. 49–56.
- [54] U. Ruhrmair, X. Xu, J. Sölter, A. Mahmoud, M. Majzoobi, F. Koushanfar, and W. Burleson, "Efficient power and timing side channels for physical unclonable functions," in *CHES*. Springer, 2014, pp. 476–492.
- [55] S. Tajik, E. Dietz, S. Frohmann, J.-P. Seifert, D. Nedospasov, C. Helfmeier, C. Boit, and H. Dittrich, "Physical characterization of arbiter PUFs," in *CHES*. Springer, 2014, pp. 493–509.
- [56] C. Boit, S. Tajik, P. Scholz, E. Amini, A. Beyreuther, H. Lohrke, and J. Seifert, "From IC debug to hardware security risk: The power of backside access and optical interaction," in *Proc. IEEE Int. Symp. Physical and Failure Analysis of Integrated Circuits*, 2016, pp. 365–369.

- [57] A. Wild, G. T. Becker, and T. Güneysu, "A fair and comprehensive large-scale analysis of oscillation-based PUFs for FPGAs," in *27th Int. Conf. FPL*, 2017, pp. 1–7.
- [58] R. Hesselbarth, F. Wilde, C. Gu, and N. Hanley, "Large scale RO PUF analysis over slice type, evaluation time and temperature on 28nm Xilinx FPGAs," in *HOST*, 2018, pp. 126–133.
- [59] J. Tobisch and G. T. Becker, "On the scaling of machine learning attacks on PUFs with application to noise bifurcation," in *International Workshop on Radio Frequency Identification: Security and Privacy Issues*. Springer, 2015, pp. 17–31.
- [60] J. Delvaux, D. Gu, D. Schellekens, and I. Verbauwhede, "Helper data algorithms for PUF-based key generation: Overview and analysis," *IEEE Trans. Comput.-Aided Design Integr. Circuits Syst.*, vol. 34, no. 6, pp. 889–902, 2015.
- [61] G. T. Becker, "Robust fuzzy extractors and helper data manipulation attacks revisited: Theory vs practice," *IEEE Trans. Dependable Secure Comput.*, 2017, DOI:10.1109/TDSC.2017.2762675.
- [62] S. T. C. Konigsmark, D. Chen, and M. D. Wong, "PolyPUF: Physically secure self-divergence," *IEEE Trans. Comput.-Aided Design Integr. Circuits Syst.*, vol. 35, no. 7, pp. 1053–1066, 2016.
- [63] J. Ye, Y. Hu, and X. Li, "RPUF: Physical unclonable function with randomized challenge to resist modeling attack," in *AsianHOST*. IEEE, 2016, pp. 1–6.
- [64] T. Idriss and M. Bayoumi, "Lightweight highly secure puf protocol for mutual authentication and secret message exchange," in *Int. Conf. RFID Technology & Application*. IEEE, 2017, pp. 214–219.
- [65] A.-R. Sadeghi, I. Visconti, and C. Wachsmann, "Enhancing rfid security and privacy by physically unclonable functions," in *Towards Hardware-Intrinsic Security*. Springer, 2010, pp. 281–305.
- [66] Y. Gao, H. Ma, S. F. Al-Sarawi, D. Abbott, and D. C. Ranasinghe, "PUF-FSM: A controlled strong PUF," *IEEE Trans. Comput.-Aided Design Integr. Circuits Syst.*, vol. 37, no. 5, pp. 1104–1108, 2018.
- [67] A. Van Herrewege, S. Katzenbeisser, R. Maes, R. Peeters, A.-R. Sadeghi, I. Verbauwhede, and C. Wachsmann, "Reverse fuzzy extractors: Enabling lightweight mutual authentication for PUF-enabled RFIDs," in *Financial Cryptography and Data Security*. Springer, 2012, pp. 374–389.
- [68] R. Maes and V. van der Leest, "Countering the effects of silicon aging on SRAM PUFs," in *HOST*. IEEE, 2014, pp. 148–153.
- [69] C. Q. Liu, Y. Cao, and C. H. Chang, "ACRO-PUF: A low-power, reliable and aging-resilient current starved inverter-based ring oscillator physical unclonable function," *IEEE Trans. Circuits and Syst. I: Reg. Papers*, vol. 64, no. 12, pp. 3138–3149, 2017.
- [70] M. S. Kirkpatrick and E. Bertino, "Software techniques to combat drift in PUF-based authentication systems," in *Workshop on Secure Component and System Identification*, 2010, p. 9.
- [71] R. Maes, V. Rožić, I. Verbauwhede, P. Koeberl, E. Van der Sluis, and V. Van der Leest, "Experimental evaluation of physically unclonable functions in 65 nm CMOS," in *Proc. ESSCIRC*. IEEE, 2012, pp. 486–489.
- [72] K.-H. Chuang, E. Bury, R. Degraeve, B. Kaczer, G. Groeseneken, I. Verbauwhede, and D. Linten, "Physically unclonable function using CMOS breakdown position," in *Proc. IEEE Int. Reliab. Phys. Symp*, 2017, DOI:10.1109/IRPS.2017.7936312.
- [73] W. Che, J. Plusquellic, and S. Bhunia, "A non-volatile memory based physically unclonable function without helper data," in *ICCAD*, 2014, pp. 148–153.
- [74] R. S. Khan, N. Noor, C. Jin, J. Scoggin, Z. Woods, S. Muneer, A. Ciardullo, P. H. NGUYEN, A. GOKIRMAK, M. van Dijk *et al.*, "Phase change memory and its applications in hardware security," in *Security Opportunities in Nano Devices and Emerging Technologies*. CRC Press, 2017, pp. 115–136.
- [75] R. Maes, A. Van Herrewege, and I. Verbauwhede, "PUFKY: A fully functional PUF-based cryptographic key generator," in *CHES*, 2012, pp. 302–319.
- [76] G. T. Becker, R. Kumar *et al.*, "Active and passive side-channel attacks on delay based PUF designs." *IACR Cryptology ePrint Archive*, vol. 2014, p. 287, 2014.
- [77] W. Yan, F. Tehranipoor, and J. A. Chandy, "PUF-based fuzzy authentication without error correcting codes," *IEEE Trans. Comput.-Aided Design Integr. Circuits Syst.*, vol. 36, no. 9, pp. 1445–1457, 2016.
- [78] E. Öztürk, G. Hammouri, and B. Sunar, "Towards robust low cost authentication for pervasive devices," in *PerCom*. IEEE, 2008, pp. 170–178.
- [79] Y. Gao, Y. Su, L. Xu, and D. C. Ranasinghe, "Lightweight (reverse) fuzzy extractor with multiple reference PUF responses," *IEEE Trans. Inf. Forensics Security*, vol. 14, no. 7, pp. 1887–1901, 2019.
- [80] Y. Su, Y. Gao, M. Chesser, O. Kavehei, A. Sample, and D. Ranasinghe, "Secucode: Intrinsic PUF entangled secure wireless code dissemination for computational RFID devices," *IEEE Trans. Dependable Secure Comput.*, 2019.
- [81] Y. Su, Y. Gao, O. Kavehei, and D. C. Ranasinghe, "Hash functions and benchmarks for resource constrained passive devices: A preliminary study," in *PerCom Workshops*. IEEE, 2019, pp. 1020–1025.

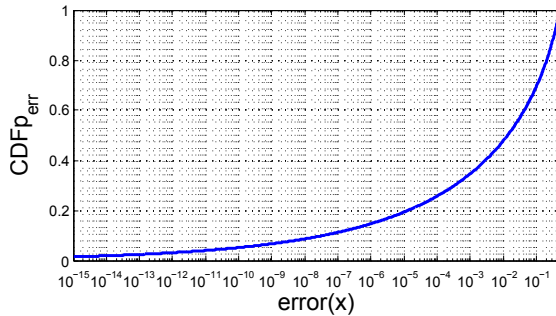


Fig. 13. Plot of $CDF_{p_{err}}(x)$ in Eq(8) as a function of error probability x .

TABLE 5
FRR_d of the ROPUF under different operating conditions and $m = 12, 14, 16$ settings, where $k = 64$ and $d = 10$.

m	25°C, 0.96 V	25°C, 1.08 V	65°C, 1.20 V	25°C, 1.32 V	25°C, 1.44 V
	FRR _d	FRR _d	FRR _d	FRR _d	FRR _d
12	20.60%; 35.30%	0%; 5.09×10^{-5}	0%; $< 10^{-9}$	0%; 4.39×10^{-4}	0.10%; 16.44%
14	8.00%; 17.97%	0%; 1.4×10^{-6}	0%; $< 10^{-9}$	0%; 2.48×10^{-5}	0%; 5.71%
16	2.50%; 8.22%	0%; 2.13×10^{-8}	0%; $< 10^{-9}$	0%; 1.27×10^{-6}	0%; 1.65%

The FRR_d based on empirical evaluations and statistical analyses based on Eq(10) are listed for comparison. The format is (empirical;statistical).

APPENDIX A RESULTS OF D-AUTHENTICATION.

In Tables 5 and 6, we give empirical and statistical evaluations on the FRR_d of ROPUF and LAPUF respectively. When the $d = 10$, the FRR_d is significantly reduced. In practice, considering that the PUF operating condition vary not too much, e.g., no more than 10% voltage deviation (1.08 V-1.32 V), the d -authentication can already minimize the FRR_d to be acceptable. For example, when the $m = 16$, the FRR_d is always less than 10^{-3} .

TABLE 6
FRR_d of the LAPUF under different operating conditions and $m = 12, 14, 16$ settings, where $k = 64$ and $d = 10$.

m	25°C, 0.96 V	25°C, 1.08 V	65°C, 1.20 V	25°C, 1.32 V	25°C, 1.44 V
	FRR _d	FRR _d	FRR _d	FRR _d	FRR _d
12	88.20%; 88.09%	0.10%; 1.09%	0%; $< 10^{-9}$	0.10%; 0.10%	7.00%; 6.74%
14	78.00%; 77.47%	0%; 0.16%	0%; $< 10^{-9}$	0.10%; 6.76×10^{-5}	2.20%; 1.82%
16	64.20%; 63.30%	0%; 1.44×10^{-4}	0%; $< 10^{-9}$	0%; 2.44×10^{-6}	0.40%; 0.34%

The FRR_d based on empirical evaluations and statistical analyses based on Eq(10) are listed for comparison. The format is (empirical;statistical).

TABLE 7
 $\lambda_{1;ref}$ and ϵ_{ref} of ROPUF under different operating conditions and the $\lambda_{2;ref}$.

Operating condition	ϵ_{ref_1}	$\lambda_{1;ref_1}$	$\lambda_{2;ref_1}$	ϵ_{ref_2}	$\lambda_{1;ref_2}$	$\lambda_{2;ref_2}$
(25°C, 0.96 V)	5.20%	0.4477	-0.3276	14.20%	0.5029	-0.3613
(25°C, 1.08 V)	0.96%	0.0324	-0.3276	9.30%	0.3533	-0.3613
(65°C, 1.20 V)	6.39%	0.2389	-0.3276	3.92%	0.1961	-0.3613
(25°C, 1.32 V)	9.29%	0.4579	-0.3276	0.76%	0.0266	-0.3613
(25°C, 1.44 V)	11.09%	0.5808	-0.3276	2.24%	0.1082	-0.3613

APPENDIX B RESULTS OF MULTIPLE-REFERENCE.

We plot the ROPUF's σ_{INTRA} under nine varying operating conditions given a specific referenced operating condition in Fig. 14. Reminding that given a referenced response, higher σ_{INTRA} for the regenerated response, higher the FRR.

In Table 7, the λ_1 , λ_2 and ϵ of the ROPUF based on two referenced operating corners, ref_1 of (25°C, 1.08 V) and ref_2 of (25°C, 1.32 V), are experimentally evaluated.

In Tables 8 and 9, by using two-reference, we experimentally and statistically evaluate the FRR_{ref_1} , FRR_{ref_2} and consequently FRR_{mr} for ROPUF and LAPUF, respectively. It is obvious that the FRR_{mr} is significantly reduced. For example, in Table 2, the FRR of the ROPUF is up to 90% when a single referenced operating corner is used under the settings of $m = 12$, $k = 64$. In Table 8, the FRR_{mr} is substantially reduced to 27% when two-reference is exploited under the same m and n settings.

APPENDIX C VALIDATION WITH HOST2018 DATASET

C.1 HOST2018 Dataset

In HOST 2018, Robert *et al.* [58] released the latest ROPUF dataset collected from 217 Xilinx Artix-7 XC7A35T FPGAs, each containing a total of 6,592 ROs, comprised of six different routing paths with 550 to 1,696 instances per type. It is suggested by this work [58] that the ROPUF response generation should be from comparison of ROs under the same routing path in order to avoid bias. Therefore, we use 1,600 ROs mapped to the upper left of the FPGA (see Table 1 in [58]) under the same routing path. To be aligned with our test for Virginia dataset in Section 5.3, we only use the first 512 ROs for our TREVERSE evaluations. Out of 217 FPGAs, 50 of them are tested under six varying temperature corners: 5°C, 15°C, 25°C, 35°C, 45°C, 55°C [58]. Under each temperature, the measurement is repeated 101 times.

C.2 ROPUF Validation

Using the setting described in Section 5.3.2, 130,816 responses are generated from one ROPUF consisting of 512 ROs implemented in one FPGA. By using 25°C as the reference, the 55°C setting provides the worst operating corner exhibiting the worst unreliability; ϵ . Herein, we have sorted the worst ϵ of all 50 ROPUFs, and used the worst five ROPUFs exhibiting the highest ϵ to represent the worst-case for evaluations. To be precise, FPGA IDs of those ROPUFs are 39, 31, 47, 10, 50, and these demonstrate a worst case ϵ of 3.06%, 2.71%, 2.59%, 2.51% and 2.48%, respectively, under 55°C. Bias for these five ROPUFs are 53.25%, 51.71%, 55.76%, 55.75%, 56.09%.

We have evaluated FRR from both empirical and statistical—formal derivation expressed in equation 9)—tests. It is clear from Table 10 (ROPUF39 under operating temperature of 5°C and 55°C) and 11 (five ROPUFs under worst operating temperature of 55°C), that the statistical results from our formalized model support the empirical results obtained from the dataset. As expected, the FRR from the statistical analysis is always higher than the empirically obtained FRR since the FRR determined from the statistical

TABLE 8

FRR_M of the ROPUF under different operating conditions and $m = 8, 10, 12, 14, 16$ settings, where $k = 64$ with two references (25°C, 1.08 V) and 25°C, 1.32 V.

m	25°C, 0.96 V			65°C, 1.20 V			25°C, 1.44 V		
	(FRR _{ref1} ; FRR _{ref2} ; FRR _M)			(FRR _{ref1} ; FRR _{ref2} ; FRR _M)			(FRR _{ref1} ; FRR _{ref2} ; FRR _M)		
8	(53.32%; 99.66%; 52.45%), (69.33%; 99.60%; 69.05%)			(71.83%; 30.62%; 23.06%), (79.52%; 63.31%; 50.34%)			(97.86%; 4.85%; 4.93%), (99.24%; 19.72%; 19.57%)		
10	(39.11%; 99.23%; 39.43%), (54.13%; 99.15%; 53.67%)			(59.57%; 18.42%; 12.27%), (68.53%; 49.87%; 34.18%)			(95.76%; 1.78%; 1.68%), (98.47%; 10.38%; 10.22%)		
12	(26.90%; 98.43%; 26.64%), (42.20%; 98.35%; 41.50%)			(47.52%; 10.14%; 5.81%), (56.92%; 37.47%; 21.33%)			(92.50%; 0.69%; 0.35%), (97.31%; 6.22%; 6.05%)		
14	(17.18%; 97.29%; 17.25%), (31.15%; 97.22%; 30.28%)			(36.16%; 4.90%; 2.64%), (45.98%; 26.50%; 12.18%)			(87.85%; 0.17%; 0.06%), (95.14%; 3.75%; 3.57%)		
16	(10.26%; 95.47%; 10.63%), (21.99%; 95.03%; 20.90%)			(26.06%; 2.41%; 1.00%), (36.52%; 17.40%; 6.35%)			(82.02%; 0.07%; 0.02%), (92.36%; 2.64%; 2.44%)		

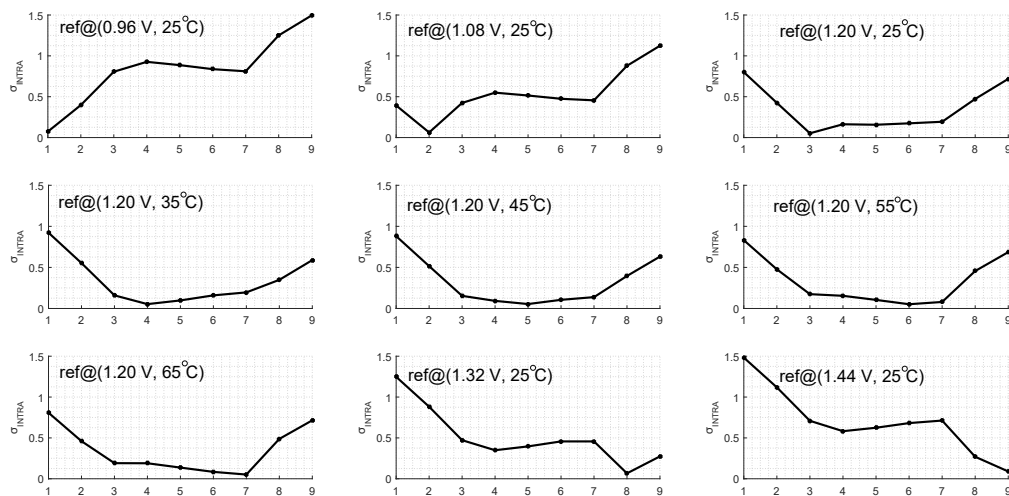
Before ‘,’ shows empirical results, after ‘,’ shows statistical results.

TABLE 9

FRR_M of the LAPUF under different operating conditions and $m = 8, 10, 12, 14, 16$ settings, where $k = 64$ with two references (25°C, 1.08 V) and (25°C, 1.32 V).

m	25°C, 0.96 V			65°C, 1.20 V			25°C, 1.44 V		
	(FRR _{ref1} ; FRR _{ref2} ; FRR _M)			(FRR _{ref1} ; FRR _{ref2} ; FRR _M)			(FRR _{ref1} ; FRR _{ref2} ; FRR _M)		
8	(82.32%; 99.99%; 83.77%), (82.21%; 99.95%; 82.16%)			(95.25%; 53.22%; 49.29%), (94.18%; 45.47%; 42.84%)			(99.85%; 11.61%; 10.39%), (99.75%; 13.73%; 13.70%)		
10	(72.70%; 99.98%; 74.53%), (72.82%; 99.90%; 72.75%)			(91.63%; 38.99%; 34.18%), (90.29%; 31.60%; 28.53%)			(99.67%; 5.22%; 4.63%), (99.40%; 7.91%; 7.86%)		
12	(61.63%; 99.98%; 63.92%), (61.24%; 99.90%; 61.19%)			(86.16%; 26.89%; 22.72%), (83.50%; 20.45%; 17.08%)			(99.37%; 2.02%; 1.80%), (98.81%; 5.00%; 4.94%)		
14	(50.23%; 99.97%; 51.84%), (49.36%; 99.89%; 49.31%)			(79.36%; 17.31%; 13.86%), (76.41%; 13.05%; 9.97%)			(98.85%; 0.72%; 0.66%), (97.70%; 3.70%; 3.61%)		
16	(39.58%; 99.94%; 41.15%), (38.19%; 99.87%; 38.14%)			(71.68%; 10.27%; 7.56%), (67.77%; 8.01%; 5.43%)			(97.87%; 0.22%; 0.21%), (96.27%; 3.06%; 2.95%)		

Before ‘,’ shows empirical results, after ‘,’ shows statistical results.



1 to 9 in x-axis sequentially stands for 9 operating conditions

(0.96 V, 25°C), (1.08 V, 25°C), (1.20 V, 25°C), (1.20 V, 35°C), (1.20 V, 45°C), (1.20 V, 55°C), (1.20 V, 65°C), (1.32 V, 25°C), (1.44 V, 25°C)

Fig. 14. ROPUF's σ_{INTRA} under nine varying operating conditions given a specific referenced operating condition.

model is a conservative estimate. This result agrees with our conclusion in Section 5.3.

We have evaluated FRR from both empirical and statistical (formal equation Eq(9)) tests. It is clear that, from Table 10 (ROPUF39 under operating temperature of 5°C and 55°C) and 11 (five ROPUFs under worst operating temperature of 55°C), statistical results from our formalized equation match empirical results. Under expectation, the statistical FRR is a conservative estimation, since it is always higher than the empirical FRR, which again agrees with our conclusion in Section 5.3.

C.3 LAPUF Validation

We have also evaluated the FRR of LAPUF adopting the settings described in Section 5.3.3. Here we use the same five

FPGA boards selected previously to obtain five LAPUFs. Table 12 summarizes the FRR of both empirical and statistical analysis—the worst ϵ is 3.10% for FPGA ID = 39. We can see that the statistical model is able to provide a conservative estimate of the FRR.

C.4 FRR with d-Authentication

Fig. 15 and 16 detail the FRR_{M,d} of ROPUFs and LAPUFs when only a single SimPUF is enrolled— $M = 1$ —and $d = 10$. For all five ROPUFs and LAPUFs, a small number of trials with $m = 17$ and $m = 18$ is able to ensure FRR_{M,d} < 10⁻⁶. This is because the ϵ of both ROPUF and LAPUF are small. Therefore, the server only needs to perform at most $2^{18} \times 10$ trials. This number of trial is}

TABLE 10

FRR of the ROPUF (HOST2018 dataset) from FPGA ID 39 under 5°C and 55°C operating conditions and m settings, where $k = 110$. The referenced operating condition is 25°C . This is the noisiest ROPUF out of the 50 tested ROPUFs.

m	5°C ($\epsilon = 2.15\%$)		55°C ($\epsilon = 3.06\%$)	
	FRR		FRR	
11	13.82%; 23.99%	35.99%; 62.71%		
12	10.28%; 19.75%	30.73%; 55.11%		
13	7.65%; 17.33%	26.13%; 47.18%		
14	5.58%; 15.40%	21.51%; 39.94%		
15	4.05%; 13.98%	17.60%; 32.35%		
16	3.05%; 13.07%	13.99%; 26.62%		
17	2.20%; 12.42%	11.01%; 20.46%		
18	1.50%; 11.89%	8.72%; 15.65%		
19	1.03%; 11.49%	6.91%; 12.21%		
20	0.75%; 11.11%	5.53%; 9.80%		

The FRR from empirical evaluations and FRR statistical analyses based on Eq(9) are listed for comparison, where the format is (empirical; statistical).

TABLE 11

FRR of the five ROPUFs (HOST2018 dataset) exhibiting the worst unreliability ϵ under the operating conditions of 55°C and m settings, where $k = 110$. Referenced operating condition is at 25°C .

m	FPGA ID = 39	FPGA ID = 31	FPGA ID = 47	FPGA ID = 10	FPGA ID = 50
	FRR ($\epsilon = 3.06\%$)	FRR ($\epsilon = 2.71\%$)	FRR ($\epsilon = 2.59\%$)	FRR ($\epsilon = 2.51\%$)	FRR ($\epsilon = 2.48\%$)
11	35.99%; 62.71%	26.06%; 56.79%	21.10%; 38.44%	20.06%; 42.40%	17.51%; 41.11%
12	30.73%; 55.11%	21.26%; 48.89%	16.32%; 31.33%	16.14%; 34.45%	13.31%; 33.41%
13	26.13%; 47.18%	16.78%; 42.43%	12.24%; 24.95%	12.48%; 28.25%	10.25%; 27.08%
14	21.51%; 39.94%	13.20%; 34.14%	9.36%; 19.91%	9.66%; 22.31%	7.47%; 21.66%
15	17.60%; 32.35%	10.40%; 26.86%	6.90%; 15.84%	7.35%; 17.97%	5.49%; 16.97%
16	13.99%; 26.62%	8.16%; 21.86%	5.13%; 13.46%	5.44%; 14.21%	3.94%; 13.98%
17	11.01%; 20.46%	6.01%; 16.85%	3.75%; 11.44%	4.17%; 11.77%	2.70%; 11.72%
18	8.72%; 15.65%	4.41%; 13.23%	2.65%; 10.16%	3.04%; 10.26%	1.95%; 10.29%
19	6.91%; 12.21%	3.35%; 10.63%	1.67%; 9.28%	2.26%; 9.23%	1.34%; 9.15%
20	5.53%; 9.80%	2.60%; 8.77%	1.16%; 8.73%	1.47%; 8.42%	0.90%; 8.50%

The FRR from empirical evaluations and FRR statistical analyses based on Eq(9) are listed for comparison, where the format is (empirical; statistical).

significantly less than the results— 2^{29} for ROPUF and 2^{31} for LAPUF in see Section 6.3—obtained from the validation using the Virginia Tech dataset exhibiting a worst case ϵ of 9.66% for ROPUF and 14.53% for LAPUF.

APPENDIX D SERVER SETTING

Table 13 summarizes the hash software implementation overhead in a resource-constraint PUF device. From Table 13, we can see that the BLAKE2s consuming least clock cycle, exhibiting best performance. Therefore, we choose BLAKE2s to be implemented in the prover side for overhead estimation. Table 15 summarizes three common GPUs in the market. Table 14 summarizes the hash function throughput/speed in the Skylake Intel CPU with a single core (Core i5-6600, 3310MHz)—latest CPU shall have a much better performance, which stands for the hash throughput of the server side. Specifically, for the chosen Blake2s, its speed of Blake2s is 648 MiBps in the server side according to Table 14.

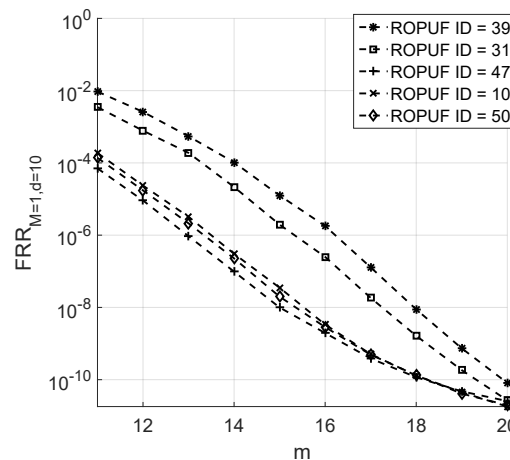


Fig. 15. The $FRR_{M,d}$ of the five noisiest ROPUF (HOST2018 dataset). Given the lower worst-case ϵ observed in this dataset compared to that from Virginia Tech [29], only a single reference response ($M=1$) from 25°C is needed. Here, $M = 1$, $d = 10$ and $k = 110$.

TABLE 12

FRR of the five LAPUF (HOST2018 dataset) under worst operating conditions of 55°C and m settings, where $k = 110$. Referenced operating condition is 25°C .

m	FPGA ID = 39	FPGA ID = 31	FPGA ID = 47	FPGA ID = 10	FPGA ID = 50
	FRR ($\epsilon = 3.10\%$)	FRR ($\epsilon = 2.93\%$)	FRR ($\epsilon = 2.52\%$)	FRR ($\epsilon = 2.66\%$)	FRR ($\epsilon = 2.71\%$)
11	44.53%; 70.40%	39.21%; 66.16%	20.40%; 41.22%	27.52%; 50.91%	27.25%; 53.92%
12	38.77%; 63.28%	33.44%; 58.39%	15.45%; 34.01%	22.07%; 42.62%	21.94%; 45.91%
13	32.78%; 57.10%	28.53%; 51.55%	11.64%; 27.14%	17.86%; 34.64%	17.43%; 38.21%
14	27.69%; 48.93%	23.79%; 43.52%	8.69%; 21.49%	14.27%; 28.89%	13.76%; 31.38%
15	22.75%; 42.15%	19.68%; 36.57%	6.57%; 17.32%	11.11%; 22.55%	10.61%; 24.51%
16	18.84%; 34.65%	15.74%; 28.97%	4.57%; 14.03%	8.67%; 17.92%	7.94%; 19.73%
17	15.64%; 28.48%	12.38%; 23.28%	3.29%; 11.67%	6.48%; 14.05%	5.91%; 15.16%
18	12.84%; 22.13%	9.96%; 18.47%	2.38%; 10.17%	4.79%; 11.56%	4.37%; 11.99%
19	10.32%; 17.34%	7.72%; 14.27%	1.69%; 9.19%	3.59%; 9.54%	3.18%; 9.85%
20	7.96%; 13.61%	6.06%; 10.77%	1.11%; 8.51%	2.59%; 8.32%	2.20%; 8.45%

The FRR from empirical evaluations and FRR statistical analyses based on Eq(9) are listed for comparison, where the format is (empirical; statistical).

APPENDIX E PROVER SETTING:

We assume for most low-end devices where the PUF is preferable, the error correction and hash operation are performed through software implementation using microcontroller due to unavailability of dedicated hardware implementation, e.g., on the FPGA platform.

Herein, we choose a MSP430FR5969 microcontroller that is usually embedded within the low-end Internet of Thing (IoT) device to evaluate the hash overhead and ECC overhead through software implementation. Thus, the overhead is measured by clock cycles. The hash software implementation overhead has been summarized in Table 13. As for the error correction code, we choose the BCH code, the reason is detailed in Section 7.2.2. In addition, we choose to implement the error correction encoding rather than the decoding in the device side, since the encoding is more lightweight than the decoding—ECC encoding and the hash form the so-called reverse fuzzy extractor (RFE) [67]. This can be clearly observed from Table 16 that summarizes the software implementation overhead of BCH encoding and decoding, regarding to the same BCH code size (n_1, k_1, t_1) or same error correction capability. Here, n_1 is the codeword

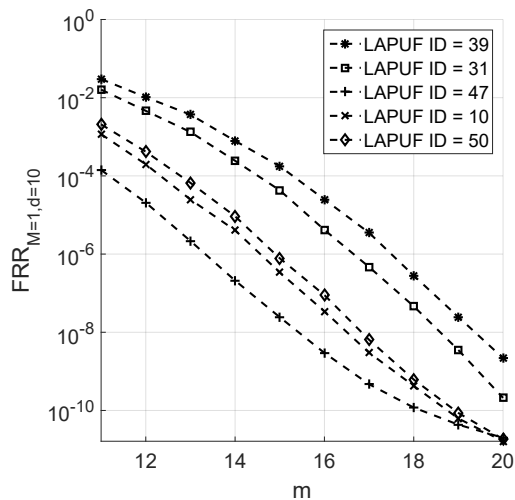


Fig. 16. The $FRR_{M=1,d}$ of five LAPUFs (HOST2018 dataset) with ($M = 1$, $d = 10$ and $k = 110$). Given the lower worst case ϵ observed in this dataset compared to that from Virginia Tech [29], only a single reference response ($M=1$) from 25°C is needed.

length, k_1 is the code size, t_1 is the errors that can be corrected within this n_1 -bit block.

It is not common to use a single large BCH block to perform error correction, which is typically split into small processing blocks to reduce implementation complexity/overhead [60], [79]. Herein, for the given example of choosing a small $BCH(n_1, k_1, t_1)$ block, to gain a security level around 110 (this number is to align with our final evaluation employing a 110-bit response, in Section 6.3), around $L = \frac{110}{k_1}$ $BCH(n_1, k_1, t_1)$ blocks are required. The failure rate of recovering a n_1 -bit response using a $BCH(n_1, k_1, t_1)$ code given a BER is expressed:

$$\mathbb{P}_1 = 1 - F_B(t_1; n_1, BER), \quad (18)$$

Given L $BCH(n_1, k_1, t_1)$ blocks are employed, the failure rate of all those BCH blocks is expressed:

$$\mathbb{P}_{\text{fail}} = 1 - (1 - \mathbb{P}_1)^L. \quad (19)$$

Table 17 summarizes the key failure rate \mathbb{P}_{fail} given different smaller $BCH(n_1, k_1, t_1)$ blocks are selected when the BER is 14.93%. This table also correspondingly evaluates the overhead of the RFE that employs the BCH encoding and the FE that employs the BCH decoding. The overhead is measured by number of clock cycles.

The clock frequency of the low-end MCU is usually several decades of MHz. For the WISP4.1DL CRFID device we evaluated, it's maximum frequency is 16MHz. However, this CRFID is batter-less and needs to save power, the clock frequency is configured to be 1MHz in practice. Therefore, one clock cycle takes 1 us to execute.

TABLE 13

Hash Overhead, evaluated using a MSP430FR5969 microcontroller embedded within the CRFID transponder, which is an intermittently powered batteryless device resembling a typical resource-constraint IoT device setting.

name	digest size	clock cycles
DM-SPECK64	64 bits	178,448
BMW-256	256 bits	150,046
SHA1	160 bits	159,969
BLAKE2s-256	256 bits	106,482
BLAKE2s-128	128 bits	104,723
SHA3-256	256 bits	584,126

Results are from [80], [81].

TABLE 14

Hash Function Speed on Skylake Intel CPU using a single core (Core i5-6600, 3310MHz).

name	speed in mebibyte per second (MiBps)
Blake2b	947
SHA-1	909
Blake2s	648
MD5	632
SHA-512	623
SHAKE-128	445
SHA-256	413
SHA3-256	367
SHA3-512	198

Reported in <https://blake2.net/>.

TABLE 15

Three Commonly Used GPU Specifications.

name	cores	clock speed	memory	price
NVIDIA Titan Xp	3840	1.6GHz	12GB GDDR5X	\$1,200
NVIDIA GTX1070	1920	1.68GHz	8GB GDDR5	\$380
AMD Radeon RX 580	2304	1.26GHz	8GB GDDR5	\$300

To perform acceleration using GPU, CUDA can be adopted.

TABLE 16

BCH code encoding and decoding overhead.

(n_1, k_1, t_1)	encoding clock cycles	decoding clock cycles
(255,123,19)	930,093	2,515,163
(255,63,30)	680,087	4,116,796
(255,47,42)	583,024	6,102,010
(255,37,45)	476,744	6,582,507
(255,29,47)	377,220	6,976,341
(255,21,55)	294,783	8,345,992
(255,9,63)	115,709	8,380,790
(511,28,111)	559,150	fail
(511,19,119)	408,127	fail

For (511,28,111) and (511,19,119) decoding, we failed to implement it in the CRFID as the computation is too heavy for the resource-constraint CRFID to handle. Part of these evaluation results are from [79] while the rest are newly evaluated.

TABLE 17

Clock cycles required of fuzzy extractor (FE) that employs BCH decoding and reverse fuzzy extractor (RFE) [67] that employs BCH encoding to tolerate a BER of 14.53%.

(n_1, k_1, t_1)	block num.	Key Failure Rate	RFE	FE
(255, 21, 55)	5	4.6×10^{-3}	1,578,638 clocks	41,834,683 clocks
(255, 9, 63)	12	7.73×10^{-5}	1,493,231 clocks	100,674,203 clocks
(511, 28, 111)	4	1.95×10^{-5}	2,341,323 clocks	fail
(511, 19, 119)	6	3.22×10^{-7}	2,553,485 clocks	fail

The key failure rate can be viewed as the false rejection rate.